THERMODYNAMIC PROPERTIES OF LIQUID IRON-CHROMIUM-OXYGEN ALLOYS

THERMODYNAMIC PROPERTIES OF LIQUID IRON-CHROMIUM-OXYGEN ALLOYS

By

STANLEY YOSHITO SHIRAISHI, B.Sc.

A Thesis

Submitted to the Faculty of Graduate Studies

in Partial Fulfilment of the Requirements

for the Degree

Master of Science

McMaster University

May 1966

MASTER OF SCIENCE (1966)
(Metallurgy)

McMASTER UNIVERSITY
Hamilton, Ontario.

TITLE: Thermodynamic Properties of Liquid Iron-Chromium-Oxygen Alloys

AUTHOR: Stanley Yoshito Shiraishi, B.Sc. (McMaster University)

SUPERVISOR: Dr. R. G. Ward

NUMBER OF PAGES: vii, 78

SCOPE AND CONTENTS:

In this thesis the equilibrium between H_2/H_2O gas mixtures and iron-chromium melts was measured over a wide range of temperatures, 1470 - 1750°C. Specimens were levitated in selected H_2/H_2O gas mixtures, quenched and analyzed for oxygen. The gas composition fixed the oxygen potential in the system and allowed the thermodynamics of the oxygen solution reaction to be determined.

Wagner interaction parameters were employed to describe the degree of chemical interaction between chromium and oxygen.

ACKNOWLEDGEMENTS

The author is indebted to his research supervisor, Dr. R. G. Ward, for suggesting the problem and his guidance and encouragement throughout the course of this work.

The author would like to thank Dr. A. McLean and Dr. N. Sano for their interest in the research and helpful discussions and Mr. D. Black for doing the oxygen analyses.

Thanks are due to the graduate students of the McMaster Metallurgy Department for their assistance on many aspects of the problem and to Miss Jennie Sabo for her skilful typing of this thesis.

The financial assistance of a National Research Council operating grant to Dr. Ward and the award of an Ontario Graduate Fellowship to the author is gratefully acknowledged.

TABLE OF CONTENTS

TABLE OF CONTENTS

TABLE OF TABLES

TABLE OF FIGURES

CHAPTER I

INTRODUCTION

Most of the chemical reactions involved in the steelmaking process are related to the removal of impurities from liquid iron and in this respect, the most active refining agent is dissolved oxygen in the melt. The oxygen required in this process may be supplied to the melt by blowing in oxygen or air, by absorption from the furnace atmosphere through the slag, or by iron oxide additions to the slag.

The chemical behaviour of the alloying elements in molten steel varies widely among the several elements commonly employed. The reactivity toward oxygen dissolved in the bath ranges all the way from the strong affinity of the deoxidizing elements, such as aluminum and zirconium to the nearly complete inertness of copper and nickel. Between these two extremes are two of the most universally used alloying elements; viz., manganese and chromium. In this investigation, the interaction of chromium with dissolved oxygen was studied. As a basis for understanding this complex behaviour, a knowledge of the activity of oxygen in pure iron is necessary.

During the past few years the levitation melting technique has been developed to the stage where it is now used extensively for melting samples under controlled atmospheres and even under the difficult conditions of high vacuum. Its use for the study of many physico-chemical problems has been achieved and reported (6, 43). Levitation was used in the present work to make an experimental study of the activity of

oxygen in liquid iron and iron-chromium alloys under controlled atmospheres of H_2 and H_2O.

Wagner's (2) interaction parameters have been used to interpret the results and determine the extent of chemical interaction between dissolved oxygen and chromium in liquid iron.

CHAPTER II

THE THERMODYNAMIC DESCRIPTION OF LIQUID METAL SOLUTIONS

1. Activity Coefficients in Multicomponent Systems

Few solutions encountered in metallurgical practice exhibit ideal behaviour. Thus it is important to know the effect of the additions of solutes 2, 3, ... to a solvent 1. Chipman et al. (1) have shown that the activity coefficient γ_2 is a function not only of its own concentration, but also of the other solutes present and γ_2 is given approximately by

$$\gamma_2 = \gamma_2^2 \times \gamma_2^3 \times \gamma_2^4 \times \ldots\ldots \qquad (1)$$

where γ_2^2 is the activity coefficient of 2 in the simple binary solution 1 – 2 containing mole fraction N_2. γ_2^3, γ_2^4, ... represent the effect of solutes 3, 4, ... on the activity coefficient of 2. The reference state for the activity coefficients is based on Henry's law so that the coefficients become equal to unity in the infinitely dilute solution, i.e., $\gamma_i = \frac{a_i}{N_i}$ where $\gamma_i \rightarrow 1$ as $N_i \rightarrow 0$.

Wagner (2) later derived an expression for the activity coefficient of component 2 in a solution containing mole fractions N_2, N_3, N_4, ... of solutes. The activity coefficient of component 2 was expressed as

$$\ln \gamma_2 (N_2, N_3, \ldots\ldots) = \ln \gamma_2^0 + N_2 \frac{\partial \ln \gamma_2}{\partial N_2} + N_3 \frac{\partial \ln \gamma_2}{\partial N_3} + \ldots\ldots$$

$$+ \frac{1}{2} N_2^2 \frac{\partial^2 \ln \gamma_2}{\partial N_2^2} + N_2 N_3 \frac{\partial^2 \ln \gamma_2}{\partial N_2 \partial N_3} + \ldots\ldots \qquad (2)$$

where the derivatives are to be taken at the limiting case of zero concentration of all solutes. The standard state is taken as the pure substance so that γ_i approaches unity as the mole fraction N_i approaches one.

If, in equation (2), the terms containing second and higher order derivatives are neglected, then the resulting relation is

$$\ln \gamma_2 \left[N_2, N_3, \ldots\right] = \ln \gamma_2^0 + N_2 \epsilon_2^2 + N_3 \epsilon_2^3 + \ldots \tag{3}$$

where the interaction coefficients ϵ_2^2, ϵ_2^3, ... are defined by

$$\epsilon_2^2 = \frac{\partial \ln \gamma_2}{\partial N_2}$$

$$\epsilon_2^3 = \frac{\partial \ln \gamma_2}{\partial N_3}$$

$$\epsilon_j^i = \left(\frac{\partial \ln \gamma_j}{\partial N_i}\right)_{N_1 \to 1} \tag{4}$$

If the standard state chosen is the infinitely dilute solution, γ_2^0 becomes unity and equation (3) becomes

$$\ln \gamma_2 \left[N_2, N_3, \ldots\right] = N_2 \epsilon_2^2 + N_3 \epsilon_2^3 + \ldots\ldots \tag{5}$$

Now it can be shown (8) that

$F_j^E = RT \ln \gamma_j$ where F^E is the excess partial molar free energy of mixing

Thus

$$F_j^E = RT \ln \gamma_j^0 + RT \sum_{i=2}^{m} \epsilon_j^i N_i \tag{6}$$

The concentrations expressed in weight percent are more convenient than mole fractions. Also, if the natural logarithms are replaced by common logarithms, then equation (5) can be rewritten

$$\log f_2 (\%2, \%3, \ldots.) = e_2^2 (\text{wt } \%2) + e_2^3 (\text{wt } \%3) + \ldots. \qquad (7)$$

where $f_j = \frac{a_j}{\%\, j}$ and the standard state for the activities is taken as the hypothetical one weight percent solution. The coefficients e_2^2, e_2^3, ..., are defined by

$$e_2^2 = \frac{\partial \log f_2}{\partial \%2}$$

$$e_2^3 = \frac{\partial \log f_2}{\partial \%3}$$

The coefficients e_j^i and ϵ_j^i are called interaction parameters and are a measure of the effect of one solute on the behaviour of another.

2. Relations Between Interaction Parameters

(i) For an infinitely dilute solution containing solutes 2 and 3, Wagner (2) has shown that the effect of 2 on the activity coefficient of 3 is related to the effect of 3 on the activity coefficient of 2 by the expression

$$\frac{\partial \ln \gamma_3}{\partial N_2} = \frac{\partial \ln \gamma_2}{\partial N_3}$$

for $N_2 = 0$, $N_3 = 0$. This alternatively can be written as

$$\epsilon_3^2 = \epsilon_2^3 \qquad (8)$$

(ii) Through the relation of weight percentage to mole fraction

and common logarithms to natural logarithms, the interaction parameter e_j^i is related to ϵ_j^i. When the solvent is iron, then

$$e_j^i = \frac{55.85}{100 \times 2.303 M_i} \epsilon_j^i$$

where M_i is the atomic weight of solute i. This equation then simplifies to the form

$$e_j^i = \frac{0.2425}{M_i} \epsilon_j^{(i)} \qquad (9)$$

Since this equation is strictly applicable only at infinite dilution, then the values obtained for ϵ_j^i from an experimental plot of log γ_j versus N_i over a wide concentration range could differ slightly from the values derived indirectly from a plot of the same data versus weight percent. The difference will be significant only when the atomic weights of the solutes are significantly different from that of iron.

This was pointed out by Schenck et al. (3), who noted that

$$\epsilon_j^i = 230 \frac{M_i}{M_1} e_j^i + \frac{M_1 - M_i}{M_1} \qquad (10)$$

The last term on the r.h.s. of equation (10) will only be significant when the molecular weight of solute i is significantly different from that of solvent 1.

(iii) The relation $M_3 e_2^3 = M_2 e_3^2$ results from the combination of equations (8) and (9). M_2 and M_3 are the atomic weights of the solutes 2 and 3. Thus

$$e_2^3 = \frac{M_2}{M_3} e_3^2 \qquad (11)$$

As with the preceding relations, this expression is strictly applicable only for infinitely dilute solutions.

3. Free Energy, Entropy and Enthalpy Interaction Parameters

Wagner's (2) treatment has been extended by Lupis and Elliott (4, 5) from consideration not only of the excess partial molar free energy, but also the excess partial molar entropy and partial molar enthalpy. In accordance with the definition of the free energy interaction parameter (equation (4)), the entropy interaction parameter is defined:

$$\sigma_j^{(i)} = \left(\frac{\partial S_j^E}{\partial N_i} \right)_{N_1 \to 1} \tag{12}$$

and the enthalpy interaction parameter is defined:

$$\eta_j^{(i)} = \left(\frac{\partial H_j^M}{\partial N_i} \right)_{N_1 \to 1} \tag{13}$$

Now Taylor expansions of S_j^E and H_j^M with terms of second and higher order derivatives omitted gives equations of the form of equation (6). These are written

$$S_j^E = S_j^{E^O} + \sum_{i=2}^{m} \sigma_j^i N_i \tag{14}$$

and

$$H_j^M = H_j^{M^O} + \sum_{i=2}^{m} \eta_j^i N_i \tag{15}$$

where the superscript O denotes the state of infinite dilution.

Now

$$F_j^E = H_j^M - TS_j^E \tag{16}$$

where F_j^E is defined by equation (6).

By substituting equations (14), (15) and (6) into relation (16)

$$RT\ \epsilon^i_j = \eta^i_j - T\sigma^i_j$$

and

$$\epsilon^i_j = \eta^i_j/RT - \sigma^i_j/R \tag{17}$$

If the enthalpy and entropy functions are approximately independent of temperature then ϵ^i_j varies linearly with the reciprocal of the absolute temperature. Also, since $\epsilon^i_j = \epsilon^j_i$, then

$$\sigma^i_j = \sigma^j_i \tag{18}$$

and

$$\eta^i_j = \eta^j_i \tag{19}$$

As pointed out in the previous section, for practical applications, weight percent instead of mole fraction is convenient. Then f_j is the activity coefficient which is employed in place of γ_j and e^i_j is the free energy interaction parameter equivalent to ϵ^i_j.

$$e^i_j = \left(\frac{\partial \log f^i_j}{\partial\ \%\ i}\right)_{\%\ 1 \to 100} \tag{20}$$

Then the free energy term expressed as the sum of entropy and enthalpy contributions is

$$2.3\ RT \log f_j = \mathcal{H}^E_j - T\mathcal{S}^E_j$$

and

$$s^i_j = \left(\frac{\partial \mathcal{S}^{E_i}_j}{\partial\ \%\ i}\right)_{\%\ 1 \to 100} \tag{21}$$

$$h_j^i = \left(\frac{\partial \mathcal{H}_j^{E_i}}{\partial \%_i} \right)_{\%1 \to 100} \tag{22}$$

Thus

$$e_j^i = \frac{h_j^i}{2.3RT} - \frac{s_j^i}{2.3R} \tag{23}$$

CHAPTER III

LITERATURE REVIEW

1. The Iron-Oxygen Solution

Oxygen in solution is important in refining liquid steel and its removal in the finishing of many grades is necessary; thus, numerous studies of its chemical behaviour in the steel bath have been made. The essential thermodynamic data required are the change in the free energy of oxygen in solution with temperature and alloy composition.

A part of the equilibrium phase diagram for the Fe – O system (8) is shown in figure 1. From this it is seen that the solution of oxygen in liquid iron is limited by the formation of a liquid iron oxide phase. A solution dilute in oxygen, e.g., 0.05 weight percent, slowly cooled, will undergo a monotectic reaction at 1528°C. The oxygen content of the liquid at the monotectic is 0.16 weight percent. This oxygen will separate out from the liquid iron as liquid iron oxide (22.6 weight percent) due to the monotectic reaction. If the rate of cooling is increased, this reaction may be suppressed and the equilibrium high temperature oxygen content of the melt will be retained in the solid state. Melts of oxygen content higher than the monotectic composition are subject to the loss of primary liquid Wustite during slow solidification.

Chipman (9) has described the solution of oxygen in liquid iron according to the reaction:

$$O_2 = 2\,\underline{O} \qquad (24)$$

where the underlined symbol represents oxygen dissolved in liquid iron.

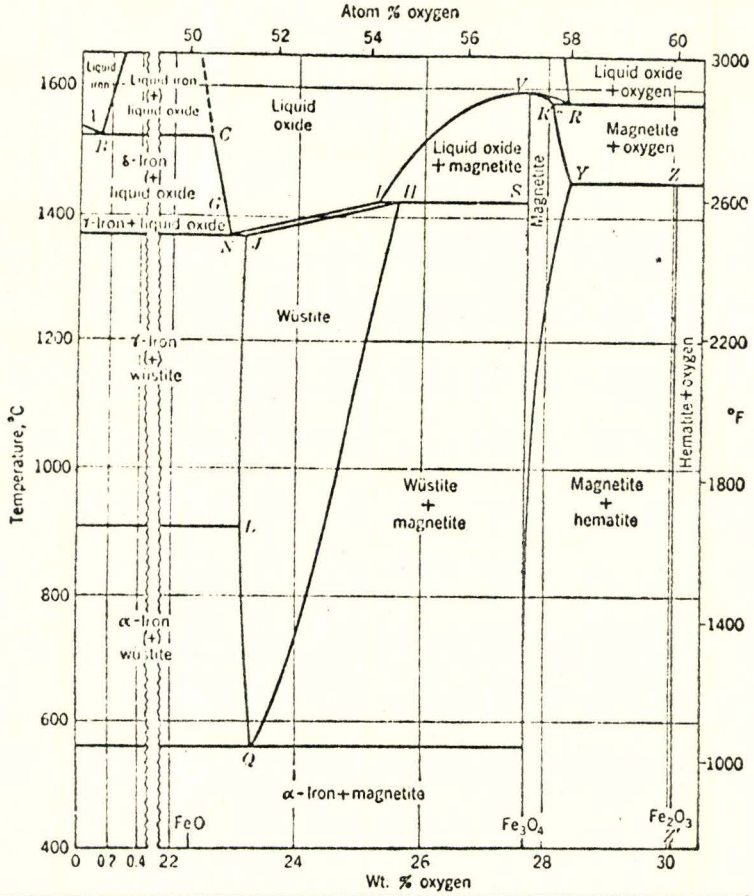

Point	°C	% O	p_{CO_2}/p_{CO}	Point	°C	% O	p_{CO_2}/p_{CO}	p_{O_2} (atm)
A	1539			*Q*	560	23.26	1.05	
B	1528	0.16	0.209	*R*	1583	28.30		1
C	1528	22.60	0.209	*R'*	1583	28.07		1
G	1400*	22.84	0.263	*S*	1424	27.64	16.2	
H	1424	25.60	16.2	*V*	1597	27.64		0.0575
I	1424	25.31	16.2	*Y*	1457	28.36		1
J	1371	23.16	0.282	*Z*	1457	30.04		1
L	911*	23.10	0.447	*Z'*		30.06		
N	1371	22.91	0.282					

* Values for pure iron

FIGURE 1

THE IRON-OXYGEN PHASE DIAGRAM

The solution of oxygen continues until at the solubility limit a liquid oxide, wustite, appears. At 1600°C this oxide forms at an oxygen pressure of approximately 10^{-8} atm, a pressure which cannot be measured directly by experiment. It is therefore necessary to use gas mixtures having a controlled oxygen potential. The most frequently used gas mixtures for this purpose are $H_2O - H_2$ and $CO_2 - CO$.

A convenient method for determining the activity and free energy of oxygen dissolved in liquid iron is based on the reaction:

$$H_2 + \underline{O} = H_2O \tag{25}$$

From the law of mass action, the equilibrium constant K may be written

$$K = \left(\frac{pH_2O}{pH_2}\right)\left(\frac{1}{a_O}\right) \tag{26}$$

$$K' = \left(\frac{pH_2O}{pH_2}\right)\left(\frac{1}{\%\ O}\right) \tag{27}$$

Chipman (9) in 1933 did one of the earliest investigations of this reaction. A small charge of electrolytic iron was melted in a high frequency furnace and equilibrated with a controlled mixture of $H_2O - H_2$ at a fixed temperature for periods up to two hours. At the end of the experiment, the melt was allowed to solidify and the oxygen content was determined by vacuum fusion analysis. The results indicated that K' was not a true constant but varied with oxygen content. Vacher (10) in his limited investigation did four experiments using a similar technique.

In a repetition of the experiments on the steam-hydrogen

equilibrium, Fontana (11) refined Chipman's experimental technique by preheating the incoming gas mixture by a platinum resistance coil in a refractory tube. He also quenched some of his melts in liquid tin in an attempt to retain the equilibrium amount of oxygen at room temperature. Oxygen dissolved in liquid iron was shown to obey Henry's law. Samarin and Chipman (12), using essentially the same technique, studied the effect of temperature on the equilibrium constant K.

In a later study by Dastur and Chipman (13), argon was added to the $H_2O - H_2$ mixture in a ratio of 4 to 1, and the inlet gases were preheated to the melt temperature. The authors stated thermal diffusion had been eliminated. On the assumption of Henrian behaviour of oxygen in liquid iron based on the earlier investigations of Fontana (11) and Samarin (12) with Chipman , Dastur calculated the temperature dependence of K over the range 1563 to 1760°C. There was no reason given by these authors for the large difference above 1700°C between their data and those of Samarin and Chipman.

The experimental method used by Gokcen (14) consisted of equilibrating 6 to 12 grams of liquid iron in alumina crucibles with $H_2O - H_2$ gas mixtures. Thermal diffusion was eliminated by bubbling the gas mixture through the melt. The argon to hydrogen ratio was kept at 4.5 to 1 in all runs to prevent hydrogen porosity in the ingots. The variation of K with temperature was examined in the range 1550 to 1700°C.

Floridis and Chipman (15) obtained data using two different experimental techniques:

(a) a technique similar to that of Dastur and Chipman (13)

but with an argon to hydrogen ratio of 6 to 1.

(b) several heats were made employing an experimental technique similar to that used by Gokcen (14).

The results were in reasonable agreement as is shown in figure 2. From their data it was concluded that the activity coefficient of oxygen and the ratio K' were not true constants. They proposed that their results were represented by the equations:

$$\log K' = 0.670 - 0.20\ (\%O) \text{ at } 1550°C \tag{28}$$

$$\log K' = 0.562 - 0.20\ (\%O) \text{ at } 1600°C \tag{29}$$

Thus, in the temperature range 1550 to 1600°C, the activity coefficient decreased with increasing concentration according to the relation

$$\log f_O = -0.20\ (\%O) \tag{30}$$

Since their data covered only a narrow range of temperature, these workers felt the best representation of the effect of temperature was a line parallel to that of Dastur and Chipman (13).

Matoba and Kuwana (20) have studied the equilibrium of oxygen in liquid iron with $H_2 - H_2O$ gaseous mixtures at 1550°, 1607° and 1663°C. Their apparatus was similar to that employed by Gokcen and Chipman (21). Their results showed that Henry's law was not applicable in the range of oxygen concentration up to 0.18 % O. These workers found that the value of $\log f_O$ decreased approximately with a linear relation as the concentration of oxygen increased, and the value of $\log f_O$ decreased

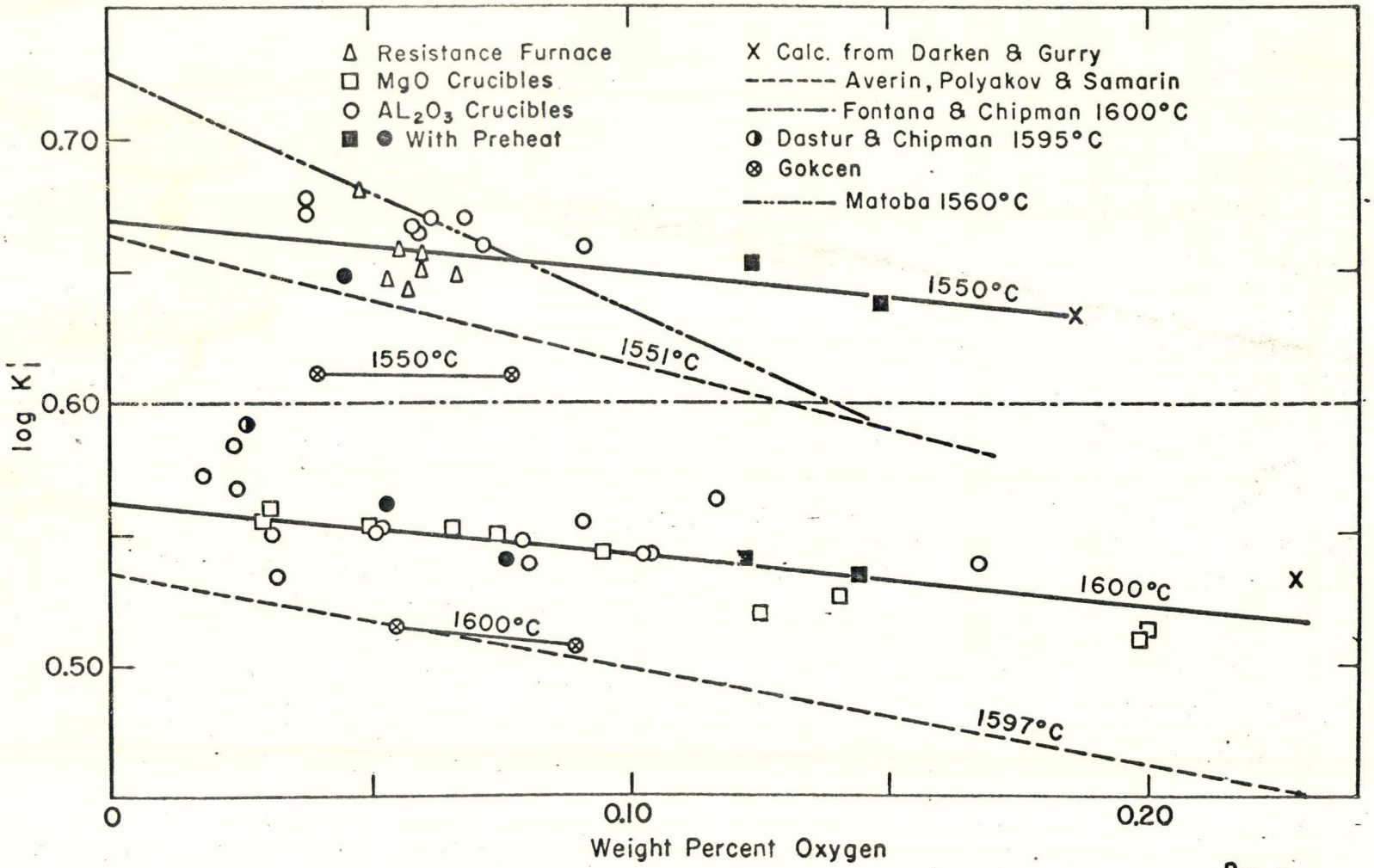

EFFECT OF OXYGEN CONCENTRATION ON EQUILIBRIUM RATIO, $K_1' = \frac{P_{H_2O}}{P_{H_2}[\%O]}$

FIGURE 2

with increasing temperature.

The interaction parameter e_O^O was shown to be a function of temperature following the equation

$$e_O^O = \frac{\partial \log f_O^O}{\partial \% O} = -10,130/T + 4.94 \qquad (31)$$

In the latest study of the steam-hydrogen equilibrium, Tankins, Gokcen and Belton (16) have shown that the dissolved oxygen in liquid iron obeys Henry's law within experimental error at 1550°C. Their experimental procedure consisted of equilibrating 10 grams of molten electrolytic iron in alumina or magnesia crucibles with $H_2O - H_2 - A$ atmospheres of known oxygen potential. The apparatus was similar to that used by Gokcen (14).

Their results for equilibrium runs at 1550°C and below 0.18 weight % oxygen were analyzed by the method of least mean squares to yield the linear variation of log K' with weight % oxygen. The resulting equation was

$$\log K' = 0.617\ (\pm 0.003) - 0.055\ (\pm 0.022)\ (\% O) \qquad (32)$$

The difference between log K' at 0% and 0.185 % $\underline{O}$ was 0.0102. An error of $\pm$ 2.5 C° in temperature measurement alone, as estimated from a plot of their data for log K' against the reciprocal of the absolute temperature, could account for this error. Thus, within the limits of experimental error, these investigators showed that K' is a true constant independent of oxygen concentration.

The aforementioned conclusions on the Henrian behaviour of

oxygen in liquid iron were in agreement with other investigations prior to 1955 with the exception of the early work of Matoba (17). Averin et al. (18) have shown a sharp decrease in log K' with oxygen but the scatter in their data does not allow calculation of an activity coefficient. The variation in K with temperature as reported by these workers was much larger than in any prior work.

Part of the work of Wriedt and Chipman (19) favors the idea of Henrian behaviour of oxygen in liquid iron since they found that the activity coefficient of oxygen was independent of oxygen content in a 75% iron - 25% nickel solution, the free energy of solution of oxygen being only slightly more positive than in pure iron.

Tankins et al. (16) have pointed out that the least squares correlation of the data of Floridis and Chipman (15) are not those presented in equations (28) and (29) but rather the following equations best represented their data:

$$\log K' = 0.6749\ (\pm\ 0.0046) - 0.228\ (\pm\ 0.064)\ (\%\ O) \text{ at } 1550°C \qquad (33)$$

$$\log K' = 0.5590\ (\pm\ 0.0070) - 0.145\ (\pm\ 0.007)\ (\%\ O) \text{ at } 1600°C \qquad (34)$$

Results in approximate agreement with equations (33) and (34) were obtained by Sakao and Sano (22) using a similar experimental technique to that of Floridis and Chipman. Matoba and Gunji (23) also used the same technique and found a much sharper dependence of log K' on the oxygen content. In many of their runs under high pH_2O/pH_2 ratios using alumina crucibles it was equivalent to working under a

liquid slag layer.

It is difficult to identify the possible sources of error causing the foregoing disagreements among various investigators because of numerous experimental difficulties inherent in high temperature equilibrium studies. Errors may be traced to:

(1) errors in oxygen analyses by the vacuum fusion method

(2) thermal diffusion

(3) uncertainties in temperature measurement

(4) quenching technique

(1) It is possible that some investigations suffered to various degrees from errors in vacuum fusion analysis of samples containing over 0.02 % O. When such samples are dropped into a graphite crucible not equipped with baffles or a lid, they can splatter on melting and yield low and erratic oxygen values thus making values of K' high and erratic.

(2) When a mixture of H_2 and H_2O encounters a thermal gradient, the heavier molecules of H_2O concentrate in the colder zone. This phenomenon called thermal diffusion has been discussed by Emmet and Schulz (24), Darken and Gurry (25), Dastur and Chipman (26), Sakao and Sano (22), and by Bockris, McKenzie and White (27) in connection with gas-metal equilibria.

A sharp temperature gradient above the melt exists when the metal is heated by induction, thus if precautions are not taken, the actual pH_2O/pH_2 ratio immediately above the melt surface may be lower than the inlet ratio used in calculating K'. Thus if thermal diffusion

prevails the measured value of K' will be larger than its true value.

(3) Errors in temperature measurements are important when the optical measurements are not calibrated within a sufficiently large range and excessive extrapolation in optical versus true temperature scale is made. The optical measurements of temperature in techniques using induction heating require emissivity and reflectivity corrections. D'Entremont (28) has shown recently that unexpected errors can arise in such measurements. The variation of the emissivity with oxygen content of the metal is not known. This may be important as a large excess surface concentration of oxygen is indicated by the known effect of oxygen in decreasing the surface tension of iron (29). Errors in temperature measurement might also occur if the window through which the metal is sighted becomes dusty or foggy.

(4) If the oxygen content of the melt is higher than 0.16 % O, the monotectic composition, then the melt is subject to the loss of primary liquid wustite if the quench rate is slow. This conclusion is applicable even to melts quenched in liquid tin or water since such quenching induces freezing from the bottom upward and is conducive to the separation of the primary liquid wustite. The gas quenching technique first introduced by Gokcen and Chipman (21) has the advantage of initiating freezing at the top surface of the melt and this will "freeze-in" the oxides.

2. The Effect of Chromium on the Activity of Dissolved Oxygen

One of the most important properties of an alloying element which is added to liquid steel is its deoxidizing power. A measure of

its deoxidizing power is the stability of the oxide with respect to that of iron. The addition of an element whose oxide is more stable than that of iron can affect the oxygen in the melt in two ways:

(1) it diminishes the amount dissolved in the steel

(2) it renders that which is in solution less active

In the early development of deoxidation theory, the first effect was most frequently studied because the actual removal of oxygen from the bath is the most important function of any deoxidizer. The second effect is equally important for those elements whose presence will affect the oxygen remaining in the solution.

The first study of the activity of oxygen in an alloyed steel bath was that of Chen and Chipman (30). Iron-chromium alloys were melted in chromic oxide and chromite crucibles under H_2O/H_2 atmospheres and held at constant temperature until equilibrium was established between the crucible, the melt and the gas phase. At the end of the heat, the melt was quenched in a stream of argon and the melt analyzed for chromium and oxygen.

A series of heats were made in alundum crucibles, the quantity of chromium charged being restricted and the gas mixture being kept less oxidizing so no solid oxide was formed. The results showed that for a given ratio of pH_2O/pH_2, low enough to prevent oxide formation, the equilibrium oxygen concentration of the bath was doubled when the chromium content was raised from zero to approximately 7 weight percent. This was equivalent to saying that the addition of 7% chromium reduced the activity coefficient of oxygen to about .5. Their results were

summarized in a subsequent paper (31) by Chipman who stated that in the range 0 to 10% chromium at 1595°C e_O^{Cr} was - 0.041.

In an attempt to minimize thermal diffusion, the gas mixture was preheated by passing it over suspended platinum wires at 1100°C. In view of subsequent investigations, it is possible the phenomenon was not eliminated. As in all crucible techniques, it is possible that oxide particles were entrapped yielding erroneous oxygen values.

Linczinskii and Samarin (32) used alumina crucibles to hold their iron-chromium melts which were equilibrated with H_2O/H_2 atmospheres. Equilibrium was reached by oxidizing chromium from the melt. They considered equilibrium was attained when the oxide phase appeared on the melt surface. This is incorrect since it may have been necessary to oxidize considerable amounts of chromium from the melt for a fixed gas composition. Thus their data may be subject to errors due to high chromium concentrations. In his paper no further experimental details were given and it is not known whether adequate precautions were taken to prevent thermal diffusion.

In his investigation of the chromium-oxygen equilibrium in liquid iron, Turkdogan (33) equilibrated iron-chromium melts, held in recrystallized alumina crucibles with chromic oxide and hydrogen-water vapor mixtures. Argon was added to the hydrogen in a ratio of 4.5:1 and the gas preheater was held at 1600°C. Experiments were conducted at 1565, 1600 and 1660°C. Some runs were conducted without any slag formation by adjusting the gas composition.

The relations between log f_O^{Cr} and the chromium content of

the iron at the temperatures 1565, 1600 and 1660°C were determined for melts with and without slag formation. Both methods gave results which were in good agreement. He also found that the activity coefficient of oxygen was independent of temperature in the range investigated. The relation between log f_O^{Cr} and percent chromium was found to be

$$\log f_O = \log f_O^{Cr} = - 0.064 \ (\% \ Cr) \qquad (35)$$

Sakao and Sano (34) have also investigated the iron-chromium oxygen equilibrium at 1600°C using iron-chromium melts up to 30 % Cr held in alumina crucibles, in contact with H_2O/H_2 atmospheres. Fifty grams of electrolytic iron were melted under argon and hydrogen and held at 1600°C, then chromium was charged. The ratio of H_2O/H_2 was fixed so that no oxide formed. The melt was then held until equilibrium when samples were sucked into silica tubes.

These workers found that the relation between log f_O^{Cr} and % Cr was not linear but followed a fairly smooth curve from 2.91 to 29.41% Cr. The calculation of f_O^{Cr} depended on the term f_O^O being unity, i.e., iron-oxygen obeyed Henry's law. These authors previously stated that iron-oxygen showed deviations from Henry's law (22) but they did not calculate an effect f_O^O since they felt their oxygen levels, which varied from 0.0173 to 0.0559 weight percent, were low enough to neglect this effect.

The data was fitted to a curve of the form

$$\log f_O^{Cr} = a \ N_{Cr} + b \ N_{Cr}^{\ x}$$

where a, b, and x are constants and N_{Cr} was the mole fraction. They

found that

$$\log f_O^{Cr} = -8.01\, N_{Cr} + 5.82\, N_{Cr}^{1.2} \text{ for } N_{Cr} < 0.3 \text{ at } 1600°C.$$

e_O^{Cr} was evaluated at 0 percent chromium and they found for chromium contents < 10% e_O^{Cr} was - 0.045. Sakao and Sano (34) also calculated an interaction parameter from the data of Linchevskii and Samarin at 1625°C and presented a plot of log f_O^{Cr} versus % Cr for their data and comparative data in the literature.

Charlton (35) has studied the solubility of oxygen in liquid iron-chromium alloys in equilibrium with an H_2O/H_2 atmosphere and either a chromite or chromic oxide crucible. A molybdenum wound resistance furnace was used and the gas mixture was bubbled through the melt. This hastened the attainment of equilibrium and eliminated thermal diffusion.

In a recent investigation by McLean and Bell (36), the equilibrium between iron-aluminum melts held in alumina crucibles with H_2O/H_2 atmospheres was studied. Some experiments were performed in which iron-chromium alloys were equilibrated with H_2O/H_2 atmospheres. The charge was electrolytic iron and pure chromium pressed into a pellet. The experimental apparatus was similar to that used by Gokcen and Chipman (21), with some modifications.

In calculating their value of e_O^{Cr} account was taken of the small amount of aluminum dissolved from the crucible. Sakao and Sano (34) in their work neglected this interaction. At 1723°C McLean and Bell determined an experimental value for e_O^{Cr} and, assuming regular solution

behaviour, calculated the value of e_O^{Cr} at 1600°C.

Matoba and Kuwana (20) have examined the effect of chromium on the activity of dissolved oxygen in liquid iron at 1550°, 1600° and 1650°C. The apparatus used was similar to that used by Gokcen and Chipman (21). Their experimental results were quite scattered but the results obtained clearly showed that the value of log f_O^{Cr} decreased almost linearly as the chromium content of the melt increased. However, they could not determine the effect of temperature for this system. The value obtained for e_O^{Cr} at 1550°, 1600° and 1650°C was - 0.0370 for chromium contents less than 12%.

Table 1 shows the results of the different investigators summarized in the form of interaction parameters.

Parameter	Chen and Chipman (30)	Turkdogan (33)	McLean and Bell (36)	Sakao and Sano (34)	Matoba and Kuwana (20)
$e_O^{Cr} = \frac{\partial \log f_O}{\partial \% Cr}$	- 0.041	- 0.064	- 0.058	- 0.045	- 0.037
$\epsilon_O^{Cr} = \frac{\partial \ln \gamma_O}{\partial N_{Cr}}$	- 8.8	- 13.7	- 12.4	- 9.65	- 3.48

Table 1

CHROMIUM-OXYGEN PARAMETERS AT 1600°C

The results listed in table 1 are plotted in figure 3.

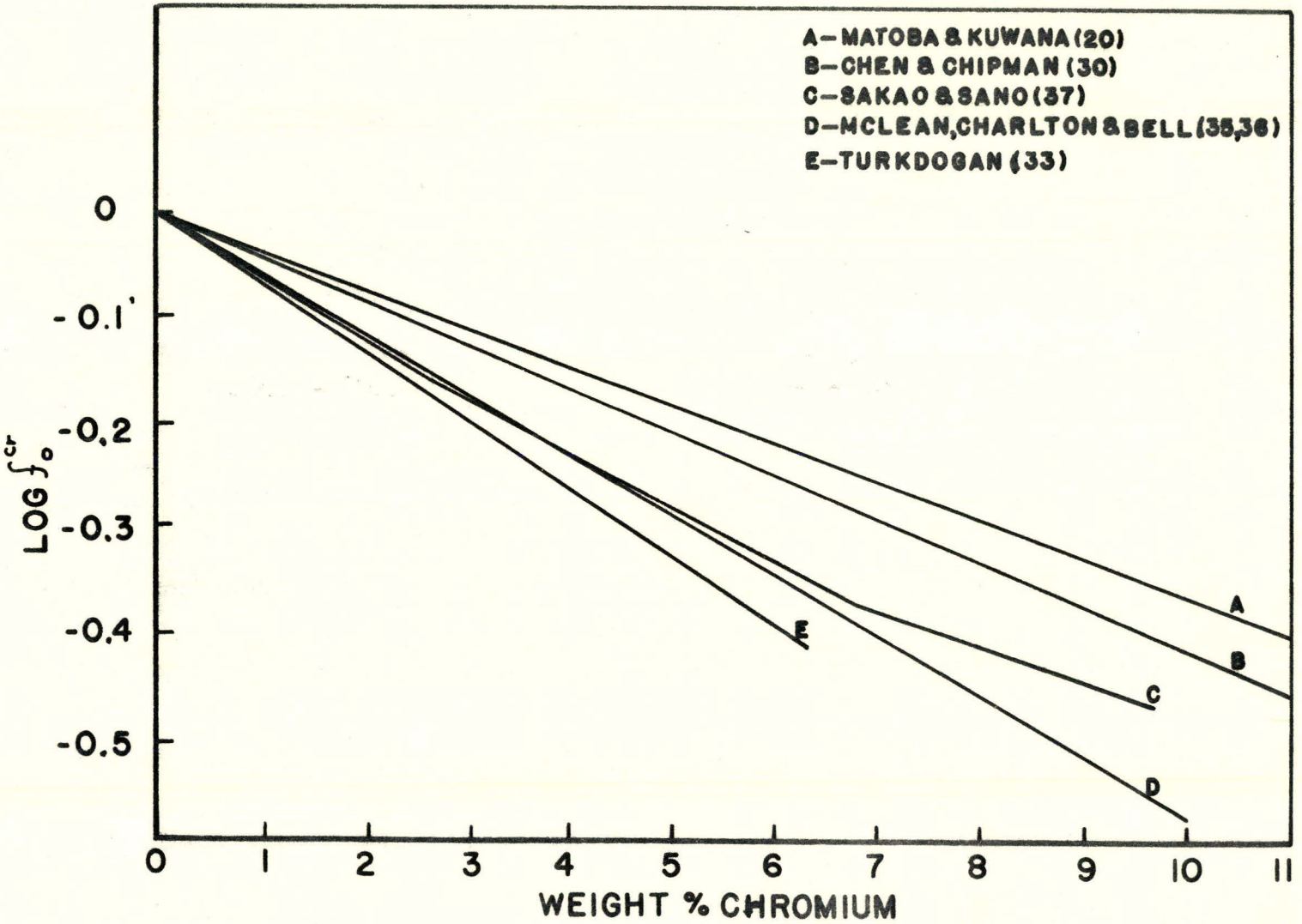

FIGURE 3

THE EFFECT OF CHROMIUM ON THE ACTIVITY COEFFICIENT OF OXYGEN IN LIQUID IRON AT 1600°C

CHAPTER IV

EXPERIMENTAL CONSIDERATIONS

1. Thermal Diffusion

If a gas mixture is held in an apparatus in which one part is hot and the other cold, the lighter component concentrates in the hotter part and the heavier one in the cold. This phenomenon is called thermal diffusion.

The degree of concentration or separation increases with increasing difference in molecular weights of the gases in the mixture and with increasing difference in temperature between the hot and cold zones. If the molecular weights are equal then it increases with increasing difference in the size of the molecules, the larger molecules concentrating in the cooler end.

Thermal diffusion was predicted by Enskog (37) in 1911, and later by Chapman (38) in 1916 in an independent work. The effect was first observed by Chapman and Dootson (39) in 1917.

Recent investigations of this phenomenon have been carried out by:

(a) Emmet and Schulz (24), who pointed out errors of as much as 40% in static atmospheres of $H_2O - H_2$ used in the early equilibrium studies

(b) Darken and Gurry (25), who described methods for minimizing thermal diffusion in $CO - CO_2$ gas mixtures flowing through a vertical furnace

(c) Dastur and Chipman (26), who investigated methods for eliminating this effect in induction heated melts with the $H_2 - H_2O$ gas mixture flowing down on the surface. Two different methods were employed by these workers:

(i) The gas mixture was preheated to minimize the steep temperature gradient existing at the gas/metal interface.

(ii) Argon was added to the gas mixture in order to increase the mean molecular weight of the mixture. This technique was based on the work of Gillespie (40) who showed that the relative separation of the two gases was inversely proportional to the square root of the mean molecular weight of the mixture.

(d) Sakao and Sano (22) who investigated the effect of argon additions to the gas mixture, preheat temperature, the distance between the preheat tube and the melt surface, and the rate of gas flow on the apparent equilibrium constant. They concluded that the effect of thermal diffusion was not as severe as mentioned by Dastur and Chipman.

(e) Richardson and Alcock (41) who discussed the effects of thermal diffusion in flowing gas mixtures. They note that failure of the gases to reach the required temperature is least likely to occur with those which have high thermal conductivities, e.g., H_2, and those which absorb strongly in the infra red, e.g., H_2O_v, although the advantage arising from these effects may not be appreciable. Alcock (42) has shown

that the thermal diffusion effect is decreased as the rate of flow of the gas mixture is increased. Richardson and Alcock concluded that if results obtained in experiments are independent of flow rate over a two to four fold range it can be taken that the phenomenon is not interfering.

In the present investigation flow rates of between 600 and 3000 cc per minute were used. At temperatures of 1688, 1725 and 1745°C, flow rates of 600, 1000 and 1350 cc per minute respectively were used.

The experimental values of log K and those predicted from equation (36) are presented in table 2.

log K from equation (36)	log K experimental	Temp. °C	Flow Rate cm^3 min^{-1}
0.420	0.400	1688	600
0.350	0.364	1725	1000
0.310	0.301	1745	1350

Table 2

The maximum difference between the log K experimental and log K from equation (36) is 0.02 at 1688°C at the lowest flow rate used. This difference is entirely accounted for by a $\pm$ 9 C° error in temperature measurement alone, which would be within the experimental error. Since at the highest temperatures studied the lower flow rates had no significant effect on the value of the equilibrium constant, it was assumed that thermal diffusion effects were negligible.

2. Temperature Control

Temperature control of the melt in levitation systems has been a major obstacle to utilizing this technique for controlled physico-chemical measurements. When a metal specimen is melted, its resistance increases and the temperature rises quickly due to I^2R losses. If the levitating force can be increased the specimen will move to a position of less field density and hence the temperature will decrease.

The factors which directly affect the levitating force and thus the temperature, for a given power supply are

(1) coil current

(2) coil geometry

(3) electrical properties of the specimen

Additional factors are

(4) sample weight

(5) gaseous environment (varying flow rate and composition)

By suitable combination of these factors, levitation can be used for many high temperature studies. A review of some of its applications is given by Peifer (43).

In the present investigation, the power was supplied to the coil by a high frequency generator, 450 kc/s and 10 k.w. In conjunction with this generator a step down transformer (7.5:1) was used to reduce the voltage and raise the amperage available to the coil.

Two different coil designs were used:

(i) a coil of Harris (44) design which gave a very high levitating force and thus was useful for low temperature runs

(ii) a coil of Jenkins (44) design which gave a lower levitating force and thus was used for high temperature runs which required fast gas flow rates

These two coil configurations are shown in figure 4.

All samples weighed approximately one gram and varying the weight was not used as a primary means for controlling the temperature.

The technique of flowing a gas atmosphere of high thermal conductivity over the specimen, which was first introduced by Jenkins (45), was used in this study. Flow rates of necessity were kept greater than 600 cc per minute as mentioned in the previous section. The reaction tube was designed to fit inside the levitating and stabilizing system in order to facilitate passing the gas over the specimen. Because of the diameter of the tube required to fit inside the coil (15 mm. i.d.), it was necessary to have a coil of high lateral stability so the droplet would not wander and hit the side. The aforementioned coils were found to fulfill this requirement.

The composition of the H_2/H_2O gas mixture was restricted somewhat because the thermal conductivity of the mixture had to be kept high, i.e., hydrogen rich. This allowed the H_2/H_2O mixtures to be used for temperature control as well as controlling the oxygen potential.

The control of temperature within the liquid specimen itself is considered to be good. Jenkins, Harris and Baker (46) have reported that in a molten metal droplet under conditions closely simulating levitation, the temperature distribution was even. This is not an unexpected observation since the melt can be seen undergoing active

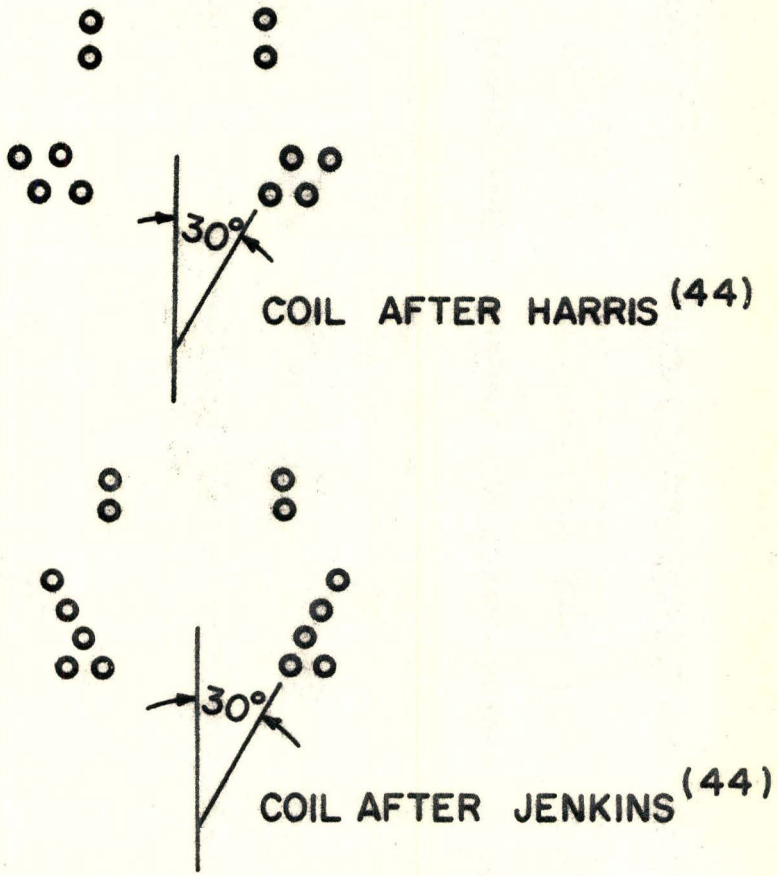

FIGURE 4

COIL CONFIGURATIONS USED IN THIS INVESTIGATION

inductive stirring during levitation.

3. Oxygen Analyses

Oxygen analyses were done with a Leco No. 734-100 analyzer. In this method, the sample is dropped into a heated graphite crucible where the oxides are reduced in the presence of excess carbon. The resulting CO, which contains all the oxygen in the sample, is then swept through the apparatus by inert helium. This CO is converted to CO_2 in passing over an oxidizing agent and is collected.

After a pre-set time the gas is released from the trap and carried by helium into a thermal conductivity cell and the change of resistance due to the thermal conductivity of CO_2 is read in "counts" on an integrator clock started at the precise time that CO_2 is passing through.

The instrument is calibrated against standard samples for counts versus percent oxygen. The accuracy of the apparatus was considered to be better than $\pm$ 10 p.p.m.

4. Temperature Measurement

Temperatures were measured using a Milletron two-colour pyrometer. Two-colour pyrometers measure the ratio of the energies of the two wavebands received from the melt and determine the temperature from the spectral characteristics of the energy distribution. The temperature measurement is independent of emissivity variations and atmospheric absorption as long as both wavebands are attenuated equally.

Single wavelength pyrometers and total radiation pyrometers measure the intensity of the radiation at the detector and are subject

to serious errors because of unknown or varying emissivities and unknown transmission characteristics of the media between the melt and the detector such as fume or dirty viewing windows. The total radiation pyrometer is also sensitive to the size of the target and the target distance since they affect the intensity of radiation received by the sensing head.

The pyrometer used in this investigation could be focussed up to three feet from the specimen surface and with the use of a closeup lens the specimen image filled the field of view with the iris fully closed. The image could be focussed at a distance of two feet.

The pyrometer was calibrated against a Pt/Pt-13%Rh thermocouple dipped into an induction heated melt of carbon saturated iron. The calibration apparatus is shown in figure 5. It consisted of a vertical vycor tube 24 in. long, 2 in. i.d., which had a lucite plate fitted on the bottom. The graphite crucible rested on an alumina tube which in turn was supported by a stainless steel tube acting also as a gas exit.

The top of the reaction tube was fitted with a rubber stopper, bored with holes to accommodate a gas inlet tube, a glass sight tube and an alumina thermocouple sheath which could be adjusted to position manually and fixed with a clamp. The optical flat and prism used to view the melt were identical to those used in the levitation experiments.

The charge of about 100 gms. of Armco iron and graphite powder were charged into the graphite crucible and the melt was heated by an induction coil connected to the high frequency generator (10 k.w., 450 kc/s). Inert helium was passed over the melt to minimize iron vapor and to

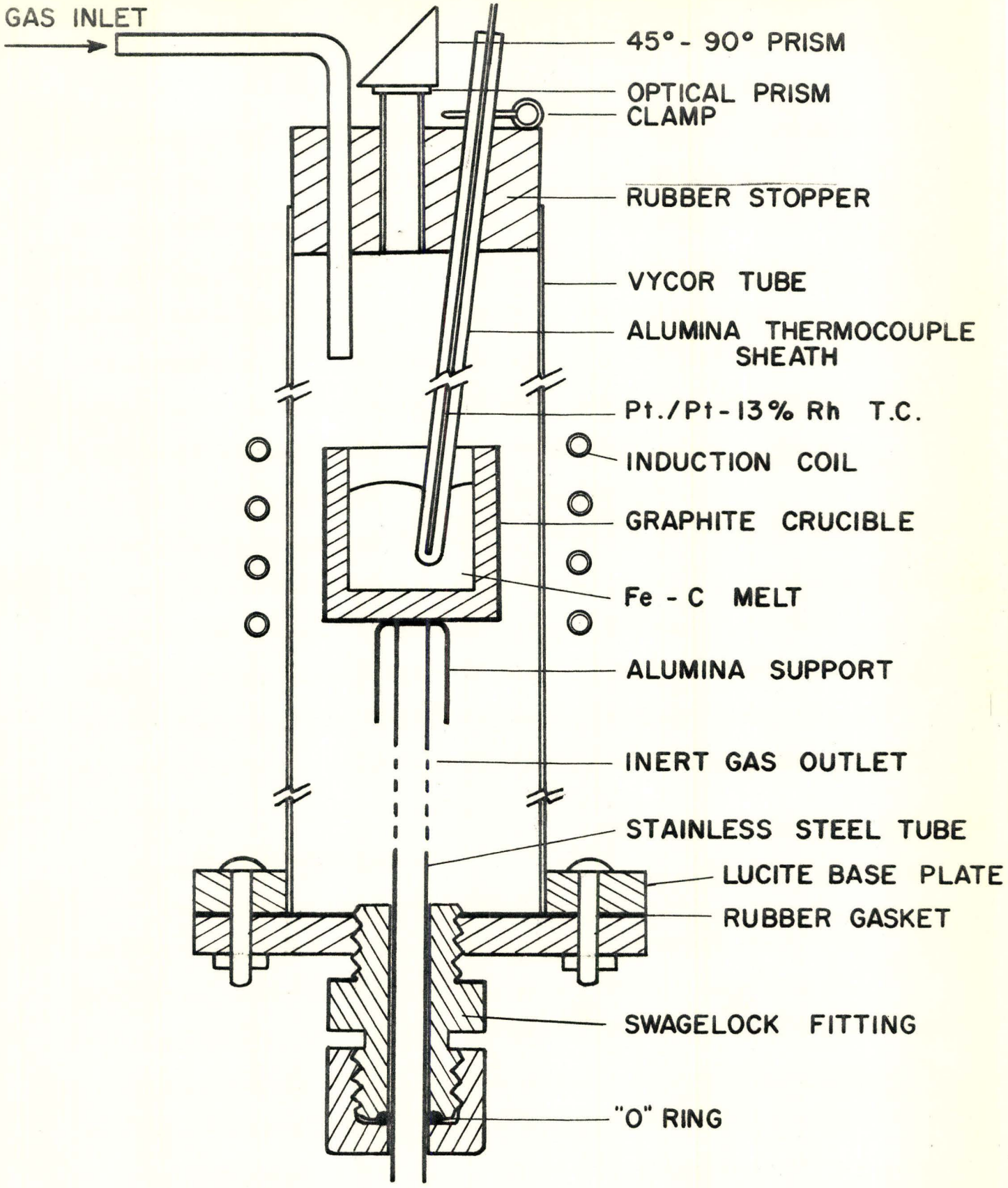

FIGURE 5

TEMPERATURE CALIBRATION APPARATUS

minimize crucible oxidation. After meltdown the thermocouple was dipped into the melt and the power input held constant until the potentiometer gave a steady reading. When this steady state was reached the potentiometer and pyrometer readings were taken simultaneously. The high frequency current had no effect on the thermocouple e.m.f. measured on the potentiometer, in agreement with Schofield and Grace (47) who found that Pt-Rh alloy thermocouple readings were unaffected by the field present in a high frequency induction coil.

Numerous readings taken on heating and cooling were in good agreement showing that there was no temperature gradient between the molten metal and the thermocouple.

The calibration curve between pyrometer temperature and thermocouple temperature is shown in figure 6. This smooth curve covered thermocouple temperatures in the range of between 1400 and 1700°C and was extrapolated to 1750°C to cover the range of temperatures in this experiment.

Although the curve obtained is strictly valid for iron-carbon melts, its use was extended to pure iron since the melting point of deoxidized Armco iron measured under levitation conditions was within $\pm$ 2 C° of the calibration curve. Similarly the melting points of iron-chromium alloys used in this investigation (less than 10%) were also within $\pm$ 10 C° of the curve and the uncertainty in temperatures obtained from figure 6, were assumed to be of the order of $\pm$ 10 C°.

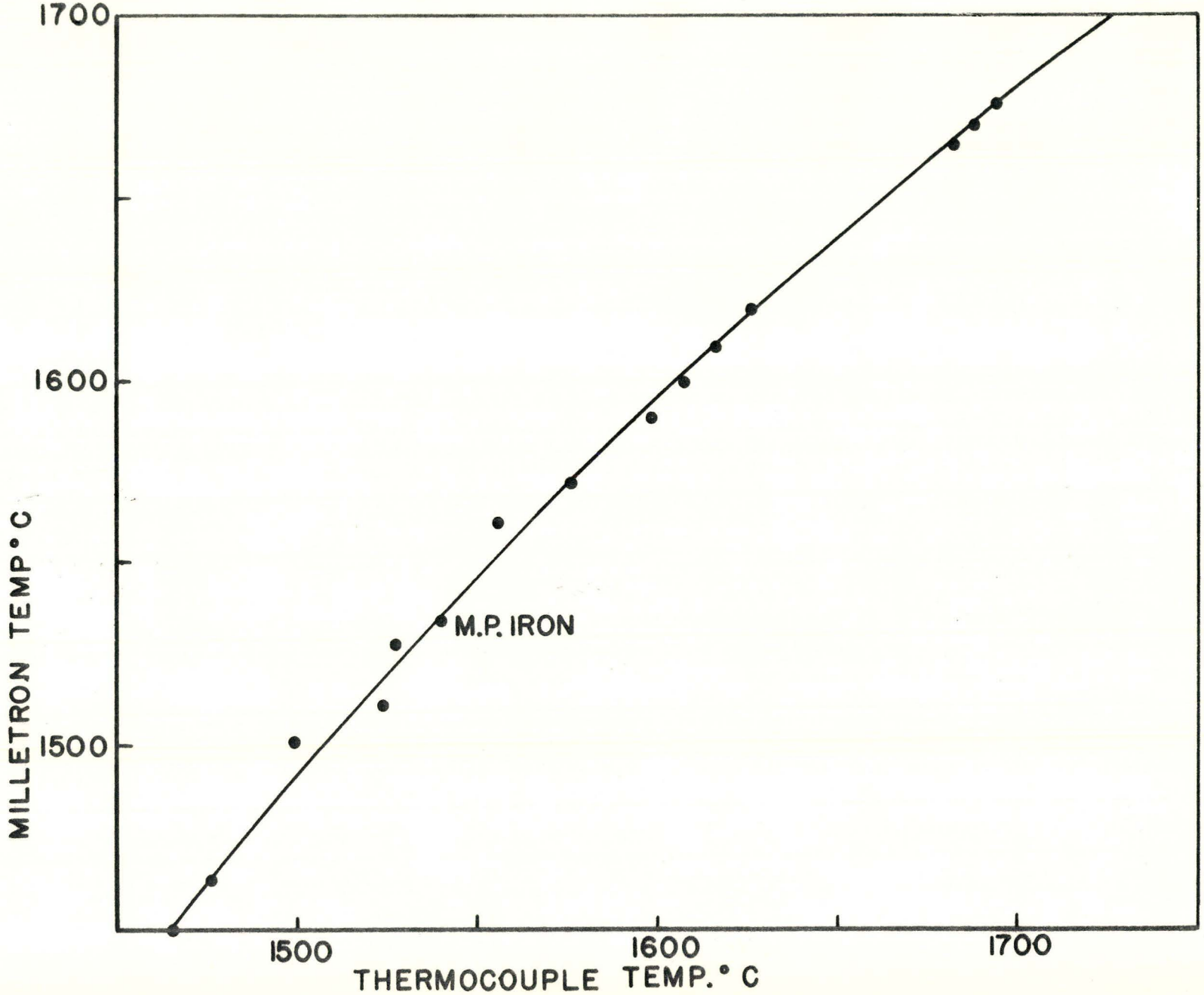

FIGURE 6

TEMPERATURE CALIBRATION CURVE

CHAPTER V

THE EXPERIMENTAL METHOD

1. The Gas System

A schematic diagram of the apparatus is shown in figure 7. Hydrogen gas was led through a platinum catalyst A, used to convert any oxygen to water vapor. From the catalytic chamber the gas was passed through magnesium perchlorate B, which removed any water vapor present.

Three two-way stopcocks H, I and J, were provided so that hydrogen could be introduced directly into the reaction tube K, and by-passing the saturator. By setting stopcock H, helium could also be passed directly into the reaction tube.

From the drying chamber, the hydrogen gas passed through a presaturator C, heated to a higher temperature than the water bath D by a hot plate so that the hydrogen was super-saturated with water vapor before it was introduced into the saturator system E. The saturators were immersed in a water bath D.

The moistened hydrogen was led by glass tubing, heated with nichrome resistance wire M, to the reaction tube. All connections were made with tygon tubing wrapped in asbestos and heated by nichrome wire.

From the gas outlet the gas passed through a wet test meter by which the flow rate and the pressure were determined. The gas was then passed to waste.

The Saturator

The saturator unit comprised six flasks as shown in figure 7.

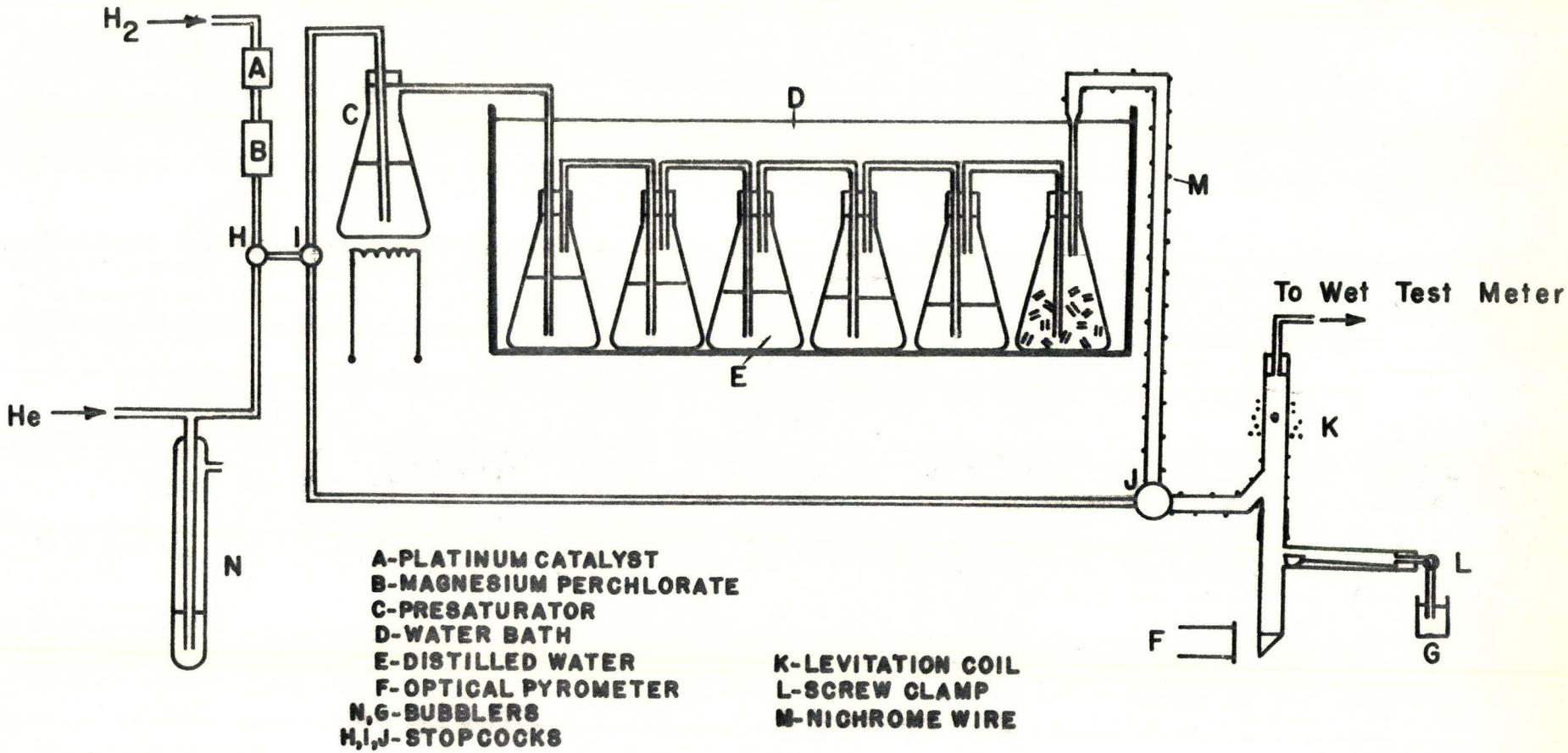

FIGURE 7

THE GAS SYSTEM

The first five were partially filled with distilled water, while the sixth was partially filled with glass raschig rings to obtain gas mixing. The flasks were weighted with lead strips wound around the outside.

The entire unit was immersed in a large water bath, the temperature of which was automatically controlled with a thermostat to $\pm$ 0.05 C° of the desired temperature.

The performance of the saturator over the range of experimental conditions was checked by weighing the water vapor absorbed in magnesium perchlorate from a measured volume of hydrogen. The observed efficiency was within $\pm$ 0.5% of the theoretical.

2. The Reaction Chamber

The reaction tube is shown in figure 8. A schematic diagram is presented in figure 9. The entire reaction assembly was constructed from vycor tubing 0.55 in. i.d. and 9 in. in length. It consisted of two separate pieces joined by a ground glass union . The upper section contained

gas inlet, A

reaction zone, C

gas outlet, D

while the lower section contained

sidearm, E

copper mould, F

gas outlet, G

optical flat, H

The copper mould (F) could be moved into the sidearm to allow

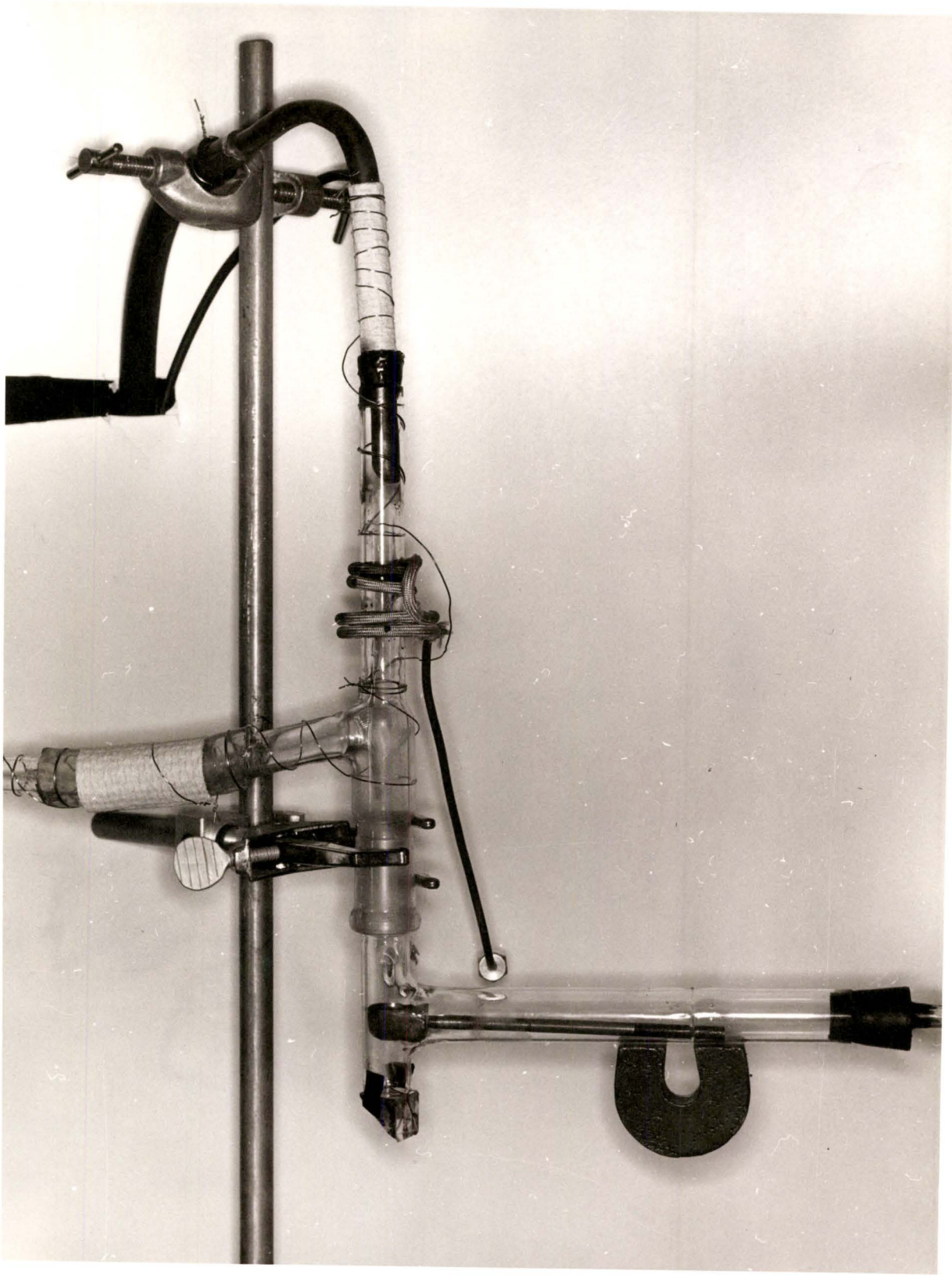

FIGURE 8

THE REACTION TUBE

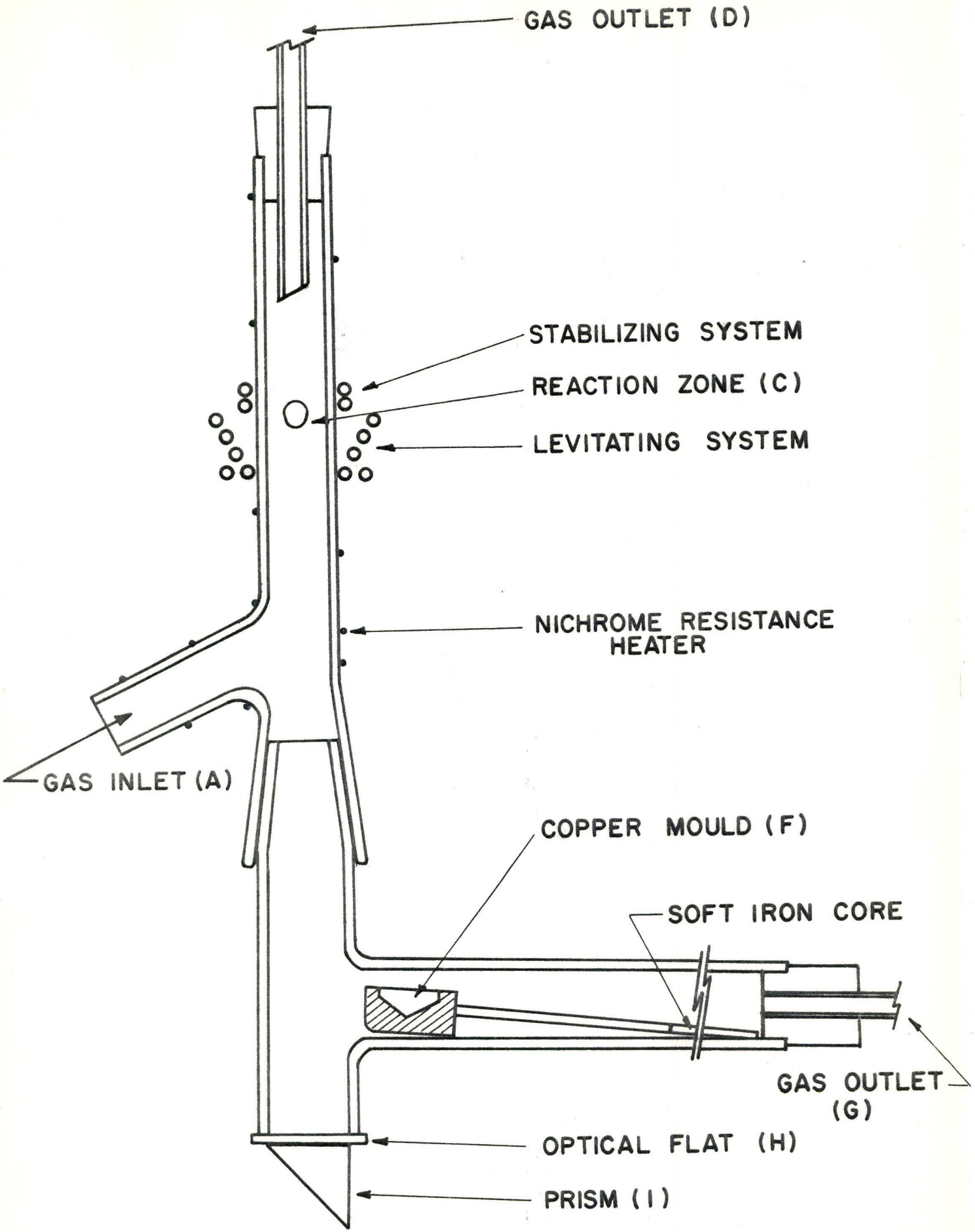

FIGURE 9
THE REACTION TUBE

the temperature measurement by viewing the bottom of the droplet through the optical flat and a 45° - 90° prism I.

The gas exit G, could be opened to purge the lower section of the reaction tube and sidearm. The gas from the sidearm was led out to a bubbler and the exit could be closed with a screw clamp.

The gas inlet A, and reaction tube were heated by a nichrome resistance wire to prevent condensation of water vapor.

3. The Quenching Technique

All samples were quenched into the mould shown in figure 10. It was constructed from a piece of copper (20 mm. x 14 mm. x 10 mm.). Brazed to it was a brass rod, on the end of which was fitted a piece of soft iron. This allowed the mould to be moved from the sidearm into position for quench with a magnet from outside the system. All samples were observed to solidify in less than one second.

4. The Materials Used

The analysis of the Armco iron used in the pure iron runs was as follows:

0.012% C

0.017% Mn

0.025% S

0.005% P

0.075% O

Samples weighing about one gram were cut from a 1/4" rod. These samples were deoxidized in dry hydrogen at about 1600°C before the equilibrium run.

FIGURE 10

THE COPPER MOULD AND A QUENCHED SPECIMEN

Iron-chromium alloys were made by carefully drilling out a hole in the Armco iron and sealing in electrolytic chromium of the following analyses:

0.015% C

0.010% S

0.040% Si

The iron-chromium samples weighing about one gram were levitated and deoxidized in neat hydrogen before equilibration with H_2 - H_2O. The alloy content was calculated from the known weights of the iron and chromium levitated.

5. The Experimental Procedure

On the day prior to experiments, the saturators were refilled with distilled water and the thermostat set at the desired temperature. Hydrogen gas was passed through the saturator and the nichrome wire heated to a temperature sufficient to prevent condensation of water vapor. The system was purged overnight.

In a typical experiment, the water bath was isolated, the hot plate heating the presaturator was turned on, and helium was passed through the reaction chamber to remove any H_2 - H_2O gas.

The bottom half of the reaction chamber was removed and the ground glass union regreased with silicone vacuum grease. The sample was then introduced into the reaction zone on the end of a mullite tube and levitated. The lower half of the reaction tube was then replaced into position and the sidearm gas exit opened to purge the entire reaction tube for five minutes.

The sample was melted by lowering the helium flow rate and the power supply and the sidearm gas exit was closed as the gas flow was changed to dry hydrogen. After deoxidation of the melt for five minutes, the gas was changed to H_2O - H_2. By adjusting the gas flow rate and power setting the desired temperature was obtained. The temperature was continuously recorded and the melt observed through the optical pyrometer. Melt temperatures were controlled to within $\pm$ 10 C° of the desired temperature.

The sample was equilibrated with the H_2 - H_2O for at least five minutes, after which it was quenched into the copper mould. The entire sample was then degreased in petroleum ether, washed in acetone, dried, weighed and stored in a dessicator until analyzed for oxygen.

CHAPTER VI

THE IRON-OXYGEN EQUILIBRIUM

1. The Activity of Oxygen in Liquid Iron

The equilibrium relationship between oxygen in liquid iron and H_2O - H_2 gas mixtures is given by the equation

$$H_2 + \underline{O} = H_2O \qquad (25)$$

for which $$K = \frac{pH_2O}{pH_2} \frac{1}{a_O}$$

i.e., $$K = \frac{pH_2O}{pH_2} \frac{1}{f_O^O \,\%\, O}$$

Defining $$K' = \frac{pH_2O}{pH_2} \frac{1}{\%\, O} \qquad (27)$$

then $$K = \frac{K'}{f_O^O}$$

where f_O^O is the activity coefficient of oxygen. The standard states are chosen so that the activity of oxygen approaches the weight percentage at infinite dilution.

In the present investigation extremely dilute iron-oxygen solutions were examined and it was assumed that Henry's law was obeyed so that K' was taken as equal to K.

Of primary interest was the relation between K and temperature. Because of the advantages inherent in the levitation melting technique, the evaluation of K at temperatures below as well as above the melting point of iron was achieved.

Results of these equilibrium experiments are shown in table 3.

Temp. °C	Melt No.	$pH_2O/pH_2 \times 10^2$	O p.p.m.	K	log K
1473	17	4.76	45	10.52	1.022
1473	15	9.52	151	6.31	0.800
1496	16	4.76	103	4.63	0.666
1498	14	9.52	147	6.47	0.811
1506	13	9.52	169	5.64	0.751
1518	7	3.41	56	6.10	0.785
1562	6	4.63	85	5.45	0.740
1592	5	6.36	145	4.39	0.642
1596	18	4.76	151	3.16	0.499
1600	4	6.36	145	4.39	0.642
1626	2	6.36	157	4.06	0.608
1644	3	6.36	186	3.42	0.534
1680	1	6.26	269	2.33	0.367
1688	8	6.38	254	2.51	0.400
1725	10	5.60	242	2.31	0.364
1745	11	5.60	280	2.00	0.301

Table 3

EQUILIBRIUM DATA FOR $K = \frac{pH_2O}{pH_2} \frac{1}{\%\ O}$

The third column in table 3 gives the ratio pH_2O/pH_2. The vapor pressure of water corresponding to each thermostatic temperature

was obtained from the steam tables. The value of pH_2 was obtained by subtracting pH_2O from the pressure over the saturator which is equal to the atmospheric pressure plus a small back pressure measured by the manometer at the gas exit. This back pressure was negligible.

The fourth column gives the amount of dissolved oxygen as determined by the Leco inert gas carrier method. The oxygen content of all samples was far below the saturation value in the liquid, thus there is little chance for loss during cooling. Segregation effects were eliminated since the entire sample was quenched and analyzed.

As stated previously, it was assumed that Henry's law was obeyed by the dissolved oxygen. If this assumption was not valid then an activity coefficient would have to be included in calculating the value of K.

Matoba and Kuwana (20) give the relation for the variation of the self interaction parameter e_O^O with temperature as

$$e_O^O = \frac{\partial \log f_O}{\partial (\% O)} = -\frac{10,130}{T} + 4.94 \qquad (31)$$

In table 4 are listed the values of e_O^O at experimental temperatures of the present investigation calculated from equation (31). Also included are the experimentally determined oxygen contents and the calculated values for the logarithm of the activity coefficient f_O.

The results of this calculation show that the maximum effect of the activity coefficient f_O is much less than the error limits placed on the oxygen analyses. Thus, in the oxygen concentration range of the present work, the error introduced by taking f_O as unity is negligible.

Temp. °C	Melt No.	O p.p.m.	e_O^O	log f_O
1473	17	45	- 0.86	- 0.004
1473	15	151	- 0.86	- 0.013
1493	16	103	- 0.80	- 0.008
1498	14	147	- 0.78	- 0.011
1506	13	169	- 0.75	- 0.013
1518	7	56	- 0.72	- 0.004
1562	6	85	- 0.58	- 0.005
1592	5	145	- 0.49	- 0.007
1596	18	151	- 0.48	- 0.007
1600	4	145	- 0.47	- 0.007
1626	2	157	- 0.39	- 0.006
1644	3	186	- 0.34	- 0.006
1680	1	269	- 0.25	- 0.007
1688	8	254	- 0.23	- 0.006
1725	10	242	- 0.13	- 0.003
1745	11	280	- 0.08	- 0.002

Table 4

LOG f_O VALUES FOR THE PRESENT INVESTIGATION

FROM THE RELATION OF MATOBA AND KUWANA

The rather low range of oxygens being dealt with (less than 300 p.p.m.) probably accounts in part for the unexpected spread in the data. The results presented in table 3 are plotted in figure 11 as log K versus 1/T.

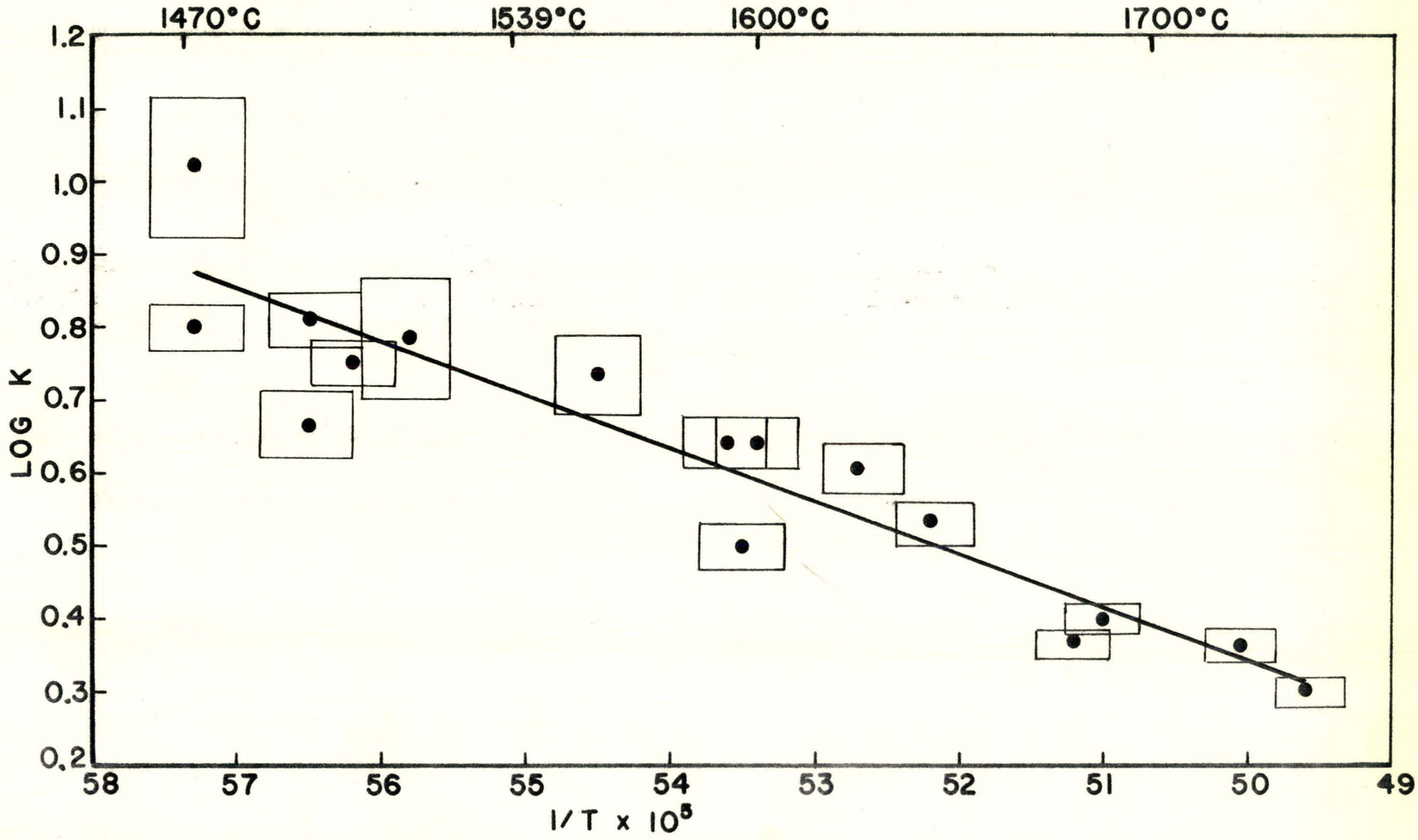

FIGURE 11

THE EFFECT OF TEMPERATURE UPON THE EQUILIBRIUM CONSTANT $K = \frac{pH_2O}{pH_2} \frac{1}{(\%\ O)}$

In figure 11 the vertical experimental error bars are equivalent to a $\pm$ 10 p.p.m. error in oxygen analysis and a slight error in determining the partial pressure of water vapor due to a $\pm$ 0.1 C° error in temperature measurement of the water bath, 0.05 C° error in temperature control of the bath and a 0.5% error in the water bath efficiency. The error in determining the partial pressure of hydrogen is negligibly small. Error in oxygen analyses is by far the most important experimental error. Also shown in figure 11 are horizontal error bars equivalent to a $\pm$ 10 C° error in temperature measurement.

The results plotted in figure 11 were analyzed by the method of least mean squares. The best straight line shown is represented by the equation

$$\log K = \frac{7159}{T} - 3.23 \qquad (36)$$

$$\Delta G^{0} = -32{,}752 + 14.78T \qquad (37)$$

The results of this investigation are compared with several other workers in table 5 and figure 12.

Authors	Log K	Temp. °C
Averin et al. (18)	9440/T - 4.536	1550 - 1700
Tankins et al. (16)	6817/T - 3.13	1550 - 1700
Sakao and Sano (22)	7040/T - 3.224	1550 - 1650
Matoba and Kuwana (20)	7480/T - 3.42	1550 - 1663
Dastur and Chipman (13)	7050/T - 3.17	1575 - 1760
Floridis and Chipman (15)	7050/T - 3.20	1550 - 1600
Present Work	7159/T - 3.23	1470 - 1750

Table 5

COMPARISON OF VARIATION OF LOG K WITH TEMPERATURE

FOR THE REACTION: $H_2 + \underline{O} = H_2O$

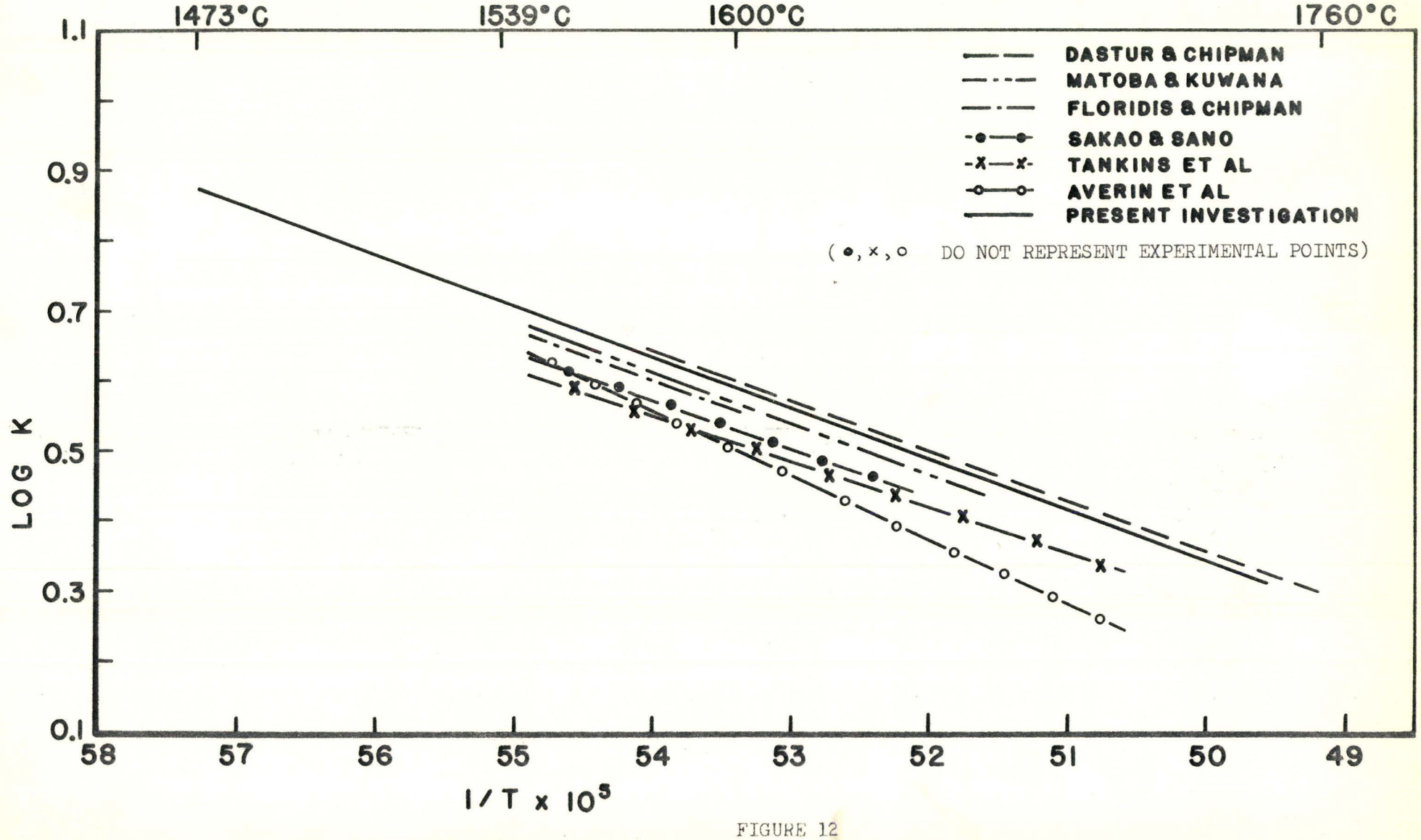

FIGURE 12

THE EFFECT OF TEMPERATURE ON THE EQUILIBRIUM CONSTANT $K = \frac{P_{H_2O}}{P_{H_2}} \frac{1}{(\%O)}$

The results of the present investigation are in good agreement with the work of Dastur and Chipman and in reasonable agreement with the work of Matoba and Kuwana.

Dastur and Chipman eliminated thermal diffusion by argon additions to the gas mixture and gas preheat. Matoba and Kuwana bubbled their gases through the melt. The agreement with these workers tends to confirm that thermal diffusion effects have been minimized.

The temperature range of the present work is the largest to date and the study of the reaction (25) has been extended 70 C° below the melting point. Within experimental error the linear relation still applies in the undercooled region.

It was decided to extend the investigation to undercooled liquid iron not only because this experiment has not been previously accomplished but also since it was experimentally more feasible to do so. In this undercooled region temperature measurement was more certain and the experiments were less susceptible to thermal diffusion effects than melts of high superheat.

2. The Free Energy of Oxygen in Liquid Iron

By combining the standard free energy changes for reaction (25) with that for the reaction

$$H_2 + \frac{1}{2} O_2 = H_2O \qquad (38)$$

$$\Delta G^0 = -59{,}905 + 13.78T \qquad \text{(J.A.N.A.F. Tables)} \qquad (39)$$

then one obtains the free energy change for the oxygen solution reaction

$$\frac{1}{2} O_2 = \underline{O} \tag{40}$$

and

$$\Delta G^O = -27{,}153 - 1.00T \tag{41}$$

3. Comparison With the Data on the Fe - C - O System

The free energy change of carbon monoxide with dissolved oxygen to form carbon dioxide, i.e.,

$$CO + \underline{O} = CO_2 \tag{42}$$

can be obtained by combining the free energy change for reaction (40) with that for the reaction

$$CO + \frac{1}{2} O_2 = CO_2 \tag{43}$$

and

$$\Delta G^O = -66{,}515 + 20.15T \tag{44}$$

Equation (44) was based on the free energies of formation of CO and CO_2 in the temperature range 1700 - 2100°K from tabulated values in "Thermochemistry for Steelmakers", volume one.

By combining equations (44) and (41), the free energy change accompanying reaction (42) is

$$\Delta G^O = -39{,}362 + 21.15T \tag{45}$$

and

$$\log K = \frac{8604}{T} - 4.62 \tag{46}$$

Several investigators have directly studied the equilibrium in reaction (42). Vacher (48), Phragmen and Kalling (49) and Marshall and Chipman (50) melted iron by induction current. Then mixtures of CO_2 - CO were equilibrated with the liquid iron.

Vacher (48) held 100 grams of iron at 1580°C and passed gases containing 10.3 to 16.6 percent CO_2 over the melt. At the end of each run the induction current was shut off to cool the melt and the ingot was sampled and analyzed for oxygen.

Phragmen and Kalling (49) used a technique essentially similar to that of Vacher. They quenched their melts by dropping a ring of iron with a small amount of aluminum in order to retain the elements dissolved in the melt.

Marshall and Chipman (50) circulated mixtures of CO_2 and CO around their furnace containing 75 to 100 grams of iron at 1540°, 1650° and 1700°C. Their melts with less than 0.02 percent carbon were allowed to cool in the furnace, but those with higher carbon were cooled after adding aluminum and allowing the induction current to stir the melt for 30 seconds. Assumption was made that aluminum preserved the carbon and oxygen which might otherwise have been lost by forming CO upon freezing.

Gokcen (14) used a resistance furnace to melt the iron and the CO - CO_2 gas was bubbled through the melt. Gokcen's data was recalculated on the basis of an activity coefficient of oxygen by Fuwa and Chipman in their review of the Fe-C-O system (63).

Only the experimental results at low carbon contents where the activity coefficient of oxygen is not being significantly affected by

the dissolved carbon can be compared with equation (46). In figure 13, the results of the various investigators are shown. The straight line represents the change in the equilibrium constant with temperature given by the equation (46) where

$$K = \frac{P_{CO_2}}{P_{CO}} \frac{1}{(\% O)} \tag{47}$$

The calculated line from thermodynamic data and results of the experimental investigation of the reaction $H_2 + \underline{O} = H_2O$ are in good agreement with the work of Vacher (48) and Marshall and Chipman (50) at all temperatures.

4. The Free Energy of Formation of Liquid Wustite

The liquid oxide phase which exists in equilibrium with solid or liquid iron has a composition given by the formula Fe_xO where the value of x is a function of temperature, and in the range considered here, is between 0.96 and 0.99. The free energy of this equilibrium phase per gram atom of oxygen can be calculated from its solubility in liquid iron. This is represented by the equation (51, 52)

$$\log \% O = - 6320T + 2.734 \tag{48}$$

This may be equally well represented by the reaction

$$Fe_xO_{\ell} = xFe_{\ell} + \underline{O} \tag{49}$$

where

$$\Delta G^{O} = 28,900 - 12.51T \tag{50}$$

When equation (50) is combined with equation (41) then one gets

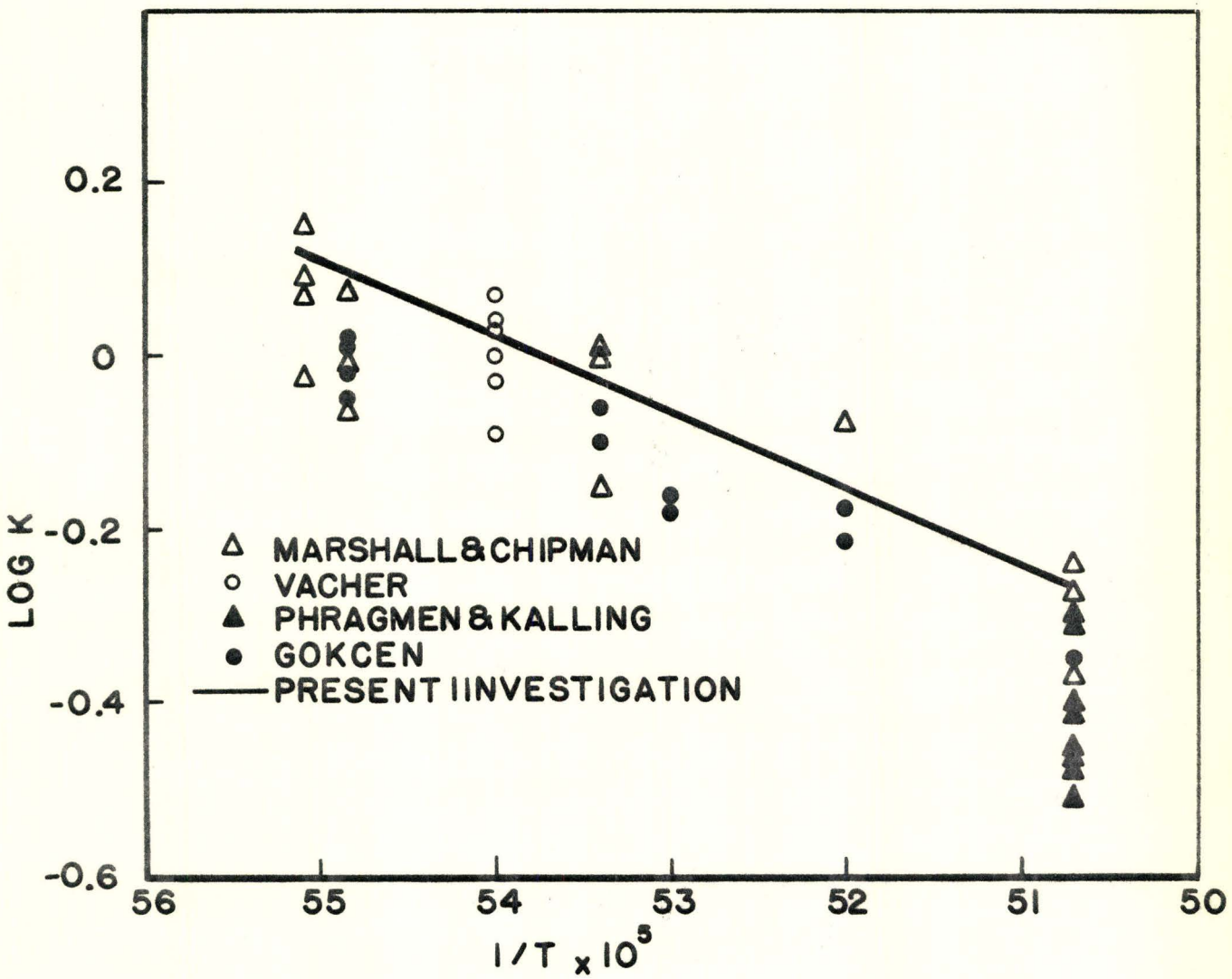

FIGURE 13

THE EFFECT OF TEMPERATURE UPON THE EQUILIBRIUM CONSTANT $K = \frac{p_{CO_2}}{p_{CO}} \frac{1}{(\% O)}$

$$xFe_{\ell} + \frac{1}{2} O_2 = Fe_xO_{\ell} \tag{51}$$

and

$$\Delta G^{O} = -56{,}053 + 11.51T \tag{52}$$

This equation represents the partial molal free energy of formation of liquid FeO of equilibrium composition. Thus the oxygen pressure of oxygen saturated liquid iron is

$$\log p_{O_2} = -\frac{24{,}504}{T} + 5.03 \tag{53}$$

The oxygen pressure of oxygen saturated liquid iron may be calculated from the experimental data of Darken and Gurry (53). These workers found the ratio of p_{CO_2}/p_{CO} in equilibrium with iron and iron oxide over a wide range of temperatures. Their data of significance in these calculations is presented in table 6.

Now the standard free energy change for the reaction

$$CO + \frac{1}{2} O_2 = CO_2 \tag{43}$$

was found to be

$$\Delta G^{O} = -66{,}515 + 20.15T \tag{44}$$

for which

$$\log K = \frac{14{,}539}{T} - 4.40 \tag{54}$$

where

$$\log K = \log \frac{p_{CO_2}}{p_{CO}} - \frac{1}{2} \log p_{O_2}$$

Values of log K as derived from equation (54) are included in table 6. From these data and the knowledge of the p_{CO_2}/p_{CO} ratio from Darken and Gurry, a value of log p_{O_2} can be computed and compared with the result of equation (53).

Temp. °C	p_{CO_2}/p_{CO}	log p_{CO_2}/p_{CO}	log K	log p_{O_2} Darken & Gurry	log p_{O_2} equation (53)
1371	0.282	- 0.550	4.44	- 9.98	------
1524	0.208	- 0.682	3.69	- 8.74	- 8.61
1575	0.194	- 0.743	3.47	- 8.43	- 8.23
1600	0.187	- 0.728	3.36	- 8.18	- 8.05

Table 6

The difference between these two series of computed oxygen pressures is very small and the present results are in good agreement with the requirements of the oxygen solubility data of Taylor and Chipman (52) and the equilibrium data of Darken and Gurry (53).

5. Summary

(i) An experimental study has been made of the equilibrium in the reaction

$$H_2 + \underline{O} = H_2O$$

over the temperature range 1470° to 1750°C using the levitation melting technique. The primary purpose was to study the reaction over a larger range of temperatures than has hitherto been examined. The study made

use of the advantages of levitation melting to examine the reaction with undercooled liquid iron.

The experimental results are represented by

$$K = \frac{pH_2O}{pH_2} \quad \frac{1}{(\%\ O)}$$

$$\log K = \frac{7159}{T} - 3.23 \qquad (36)$$

(ii) The free energy of solution of oxygen into liquid iron, i.e., the standard free energy accompanying the reaction

$$\frac{1}{2}\ O_2 = \underline{O}$$

was found to be

$$\Delta G^O = -27{,}153 - 1.00T \qquad (41)$$

(iii) The derived value of the equilibrium constant K for the reaction

$$CO + \underline{O} = CO_2$$

was calculated from the known free energies of the gases involved and free energy change in the oxygen solution reaction. The result was:

$$\log K = \frac{8604}{T} - 4.62 \qquad (46)$$

This result was found to be in good agreement with direct experimental determinations.

(iv) Related thermodynamic quantities were derived from equation (36) which substantiate the results of oxygen solubility obtained by Taylor

and Chipman and are in good agreement with the equilibrium data on the iron-oxygen system obtained by Darken and Gurry.

CHAPTER VII

CHROMIUM-OXYGEN INTERACTION IN LIQUID IRON

1. Calculation of the Interaction Parameter e_O^{Cr}

The effect of chromium on the activity coefficient of oxygen in liquid iron was determined from the reaction

$$H_2 + \underline{O} = H_2O \qquad (25)$$

where

$$K = \frac{pH_2O}{pH_2} \frac{1}{a_O}$$

and

$$K = \frac{pH_2O}{pH_2} \frac{1}{f_O \% O}$$

so that

$$K = \frac{K'}{f_O}$$

$$\log K = \log K' - \log f_O$$

where f_O is the activity coefficient of oxygen in liquid Fe-Cr-O solutions. In this case

$$f_O = f_O^O \cdot f_O^{Cr}$$

Now if f_O^O is unity as explained previously, then f_O is equal to f_O^{Cr} so that

$$\log K' = \log K + \log f_O^{Cr}$$

and

$$\log K' = e_O^{Cr} (\% Cr) + \log K \qquad (55)$$

From equation (55) it is seen that if log K' is plotted versus weight percent chromium at fixed temperature and a straight line is obtained then its slope will be the interaction parameter e_O^{Cr} and the intercept at zero weight chromium is equal to log K.

In table 7 are the results of runs in which H_2O - H_2 gas mixtures have been equilibrated with liquid iron-chromium alloys.

Temp. °C	Melt No.	$pH_2O/pH_2 \times 10^2$	O p.p.m.	% Cr	log K'
1516	27	5.65	109	1.60	0.715
1516	31	4.76	129	2.44	0.567
1516	28	5.65	144	3.50	0.594
1516	30	4.76	183	4.60	0.415
1585	26	6.37	220	1.60	0.462
1585	17	5.14	198	2.79	0.414
1585	18	5.14	230	3.15	0.349
1585	19	4.28	193	3.44	0.346
1585	20	4.28	181	3.60	0.374
1585	21	4.28	229	5.00	0.272
1726	22	6.38	377	1.43	0.229
1726	23	6.38	461	2.89	0.141
1726	24	6.38	535	3.41	0.076
1726	25	6.38	805	6.01	-0.101

Table 7

EQUILIBRIUM DATA FOR THE REACTION $H_2 + \underline{O}_{Fe-Cr} = H_2O$

$$K' = \frac{pH_2O}{pH_2} \quad \frac{1}{(\% O)}$$

In figure 14, the data for log K' and weight percent chromium from table 7 are plotted. Experimental error bars were calculated as before. Included on the graph are the values of the true equilibrium constant K for pure iron from equation (36). The gradient of each isotherm is equivalent to the interaction parameter e_O^{Cr}. The data when analyzed by the method of least mean squares yield the following equations with their probable error

At 1516°C

$$\log K' = -0.074 \pm (0.012) \% Cr + 0.791 \pm (0.029) \quad (56)$$

At 1585°C

$$\log K' = -0.068 \pm (0.005) \% Cr + 0.597 \pm (0.015) \quad (57)$$

At 1726°C

$$\log K' = -0.075 \pm (0.002) \% Cr + 0.344 \pm (0.007) \quad (58)$$

The experimental value of e_O^{Cr} at 1585°C is compared with several other investigators in table 8.

	Chen and Chipman (30)	Turkdogan (33)	Charlton (35)	Matoba and Kuwana (20)	Present Work
e_O^{Cr}	- 0.041	- 0.064	- 0.059	- 0.037	- 0.068
ϵ_O^{Cr}	- 8.8	-13.7	-12.7	- 7.9	-14.6

Table 8

CHROMIUM-OXYGEN PARAMETERS AT 1585°C

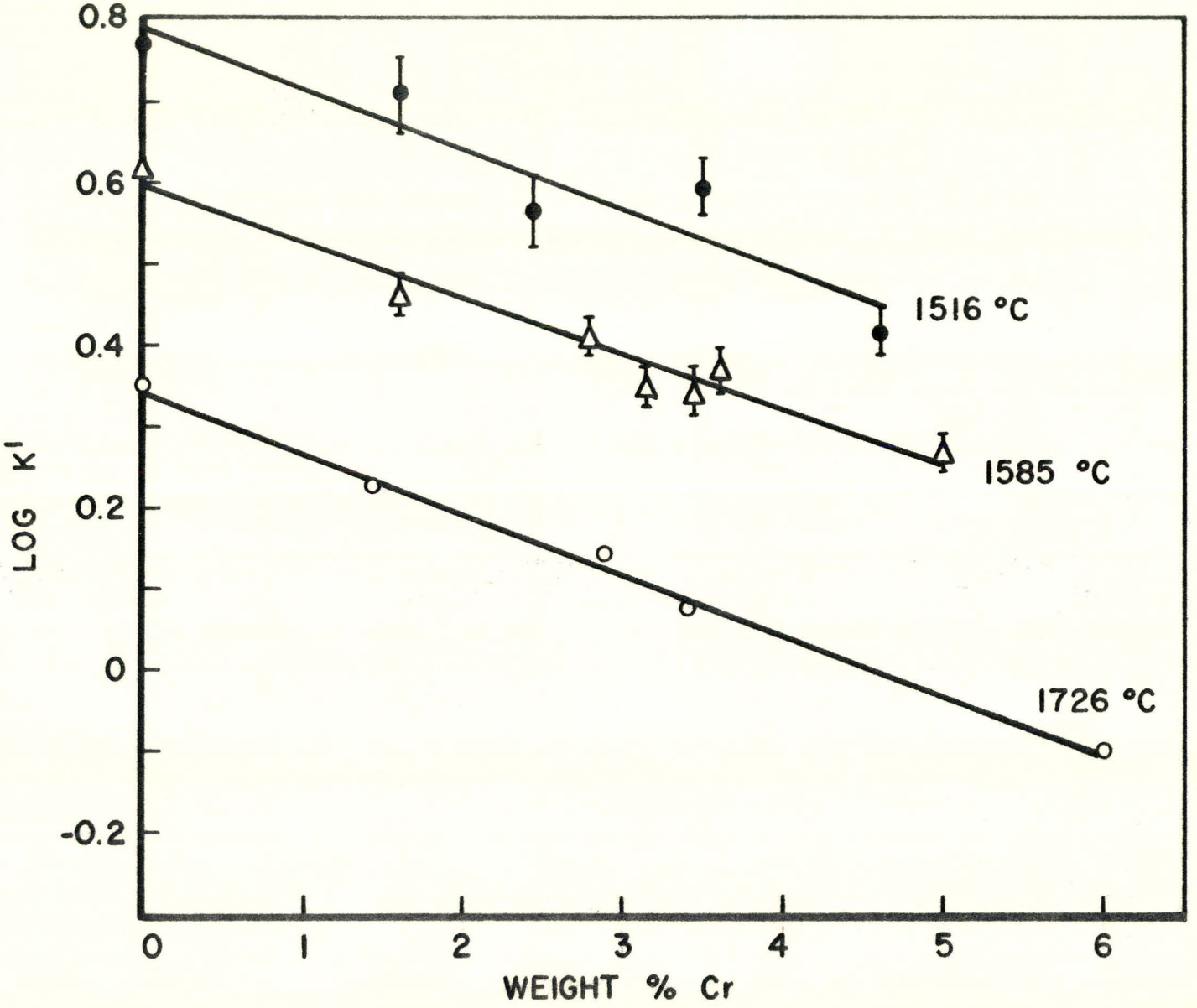

FIGURE 14

The experimental value of e_O^{Cr} at 1585°C from this investigation is in reasonable agreement with the work of Turkdogan (33) and the calculated value based on Charlton's (35) work assuming regular solution behaviour.

The negative value of the interaction parameter e_O^{Cr} shows that the activity coefficient of oxygen decreases as the chromium content is increased. This can be attributed to the greater chemical affinity of oxygen for chromium than for iron.

Ohtani and Gokcen (54) concluded after reviewing a number of Fe-O-X systems that the interaction parameter decreases with increasing stability of the compounds formed between the solutes X and O. These authors state that as a consequence of Mendeleef's law[55] there should be a relation between e_O^X and the atomic number of the solute X. In figure 15 values of e_O^X are plotted against the atomic number. In table 9 values of e_O^X plotted in figure 15 are presented.

The value of e_O^C is from the equilibrium data for $CO_2 + \underline{C} = 2\ CO$ by Marshall and Chipman (56). The result for e_O^O is zero from the work of Tankins et al. (16). For boron e_O^B is estimated from figure 15.

The values of e_O^X for Al and Si are from Gokcen and Chipman (57), P from Pearson and Turkdogan (59) all from $H_2 + \underline{O} = H_2O$; for S, from $H_2 + \underline{S} = H_2S$ by Matoba and Uno (60). For V, the parameter e_O^V is from Dastur and Chipman (61), Cr from the present investigation; Mn, Co and Ni from Thiery (62), Floridis (15) and Wriedt (63) with Chipman, all from $H_2 + \underline{O} = H_2O$. The value of Ti is estimated from figure 15.

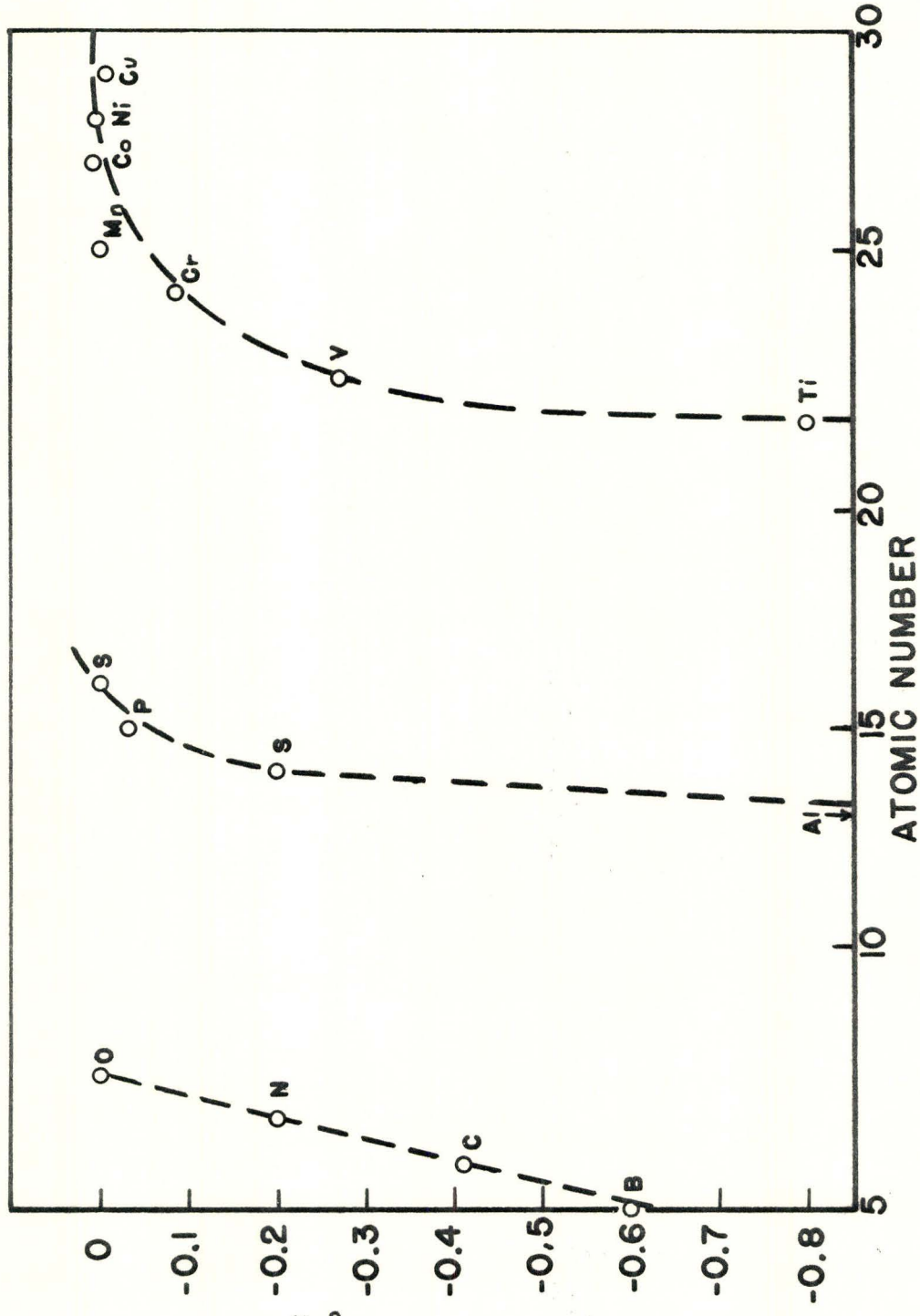
0
-0.1
-0.2
-0.3
-0.4
-0.5
-0.6
-0.7
-0.8
e_o^x
5
10
15
20
25
30
ATOMIC NUMBER
O
N
C
B
S
P
S
Al
Ti
V
Cr
Mn
Co
Ni
Cu

FIGURE 15

Solute X	ϵ_O^X	e_O^X	References	Method
B	- 27	- 0.60	fig. 15	Estimated
C	- 20	- 0.41	31, 56	$C + CO_2 = CO_2$
N	- 11.5	- 0.20	fig. 15	Estimated
O	0	0	16	$H_2 + \underline{O} = H_2O$
Al	-890 to -1340	-8 to -12	57	$H_2 + \underline{O} = H_2O$
Si	- 23	- 0.2	21, 58	$H_2 + \underline{O} = H_2O$
P	- 4	- 0.032	59	$H_2 + \underline{O} = H_2O$
S	0	0	60	$H_2 + \underline{S} = H_2S$
Ti	- 157	- 0.8	fig. 15	Estimated
V	- 57	- 0.27	61	$H_2 + \underline{O} = H_2O$
Cr	- 14.6	- 0.068	Present Work	$H_2 + \underline{O} = H_2O$
Mn	0	0	62	$H_2 + \underline{O} = H_2O$
Co	1.7	0.007	15	$H_2 + \underline{O} = H_2O$
Ni	1.4	0.006	63	$H_2 + \underline{O} = H_2O$
Cu	- 2.5	- 0.0095	15	$H_2 + \underline{O} = H_2O$

Table 9

VALUES OF ϵ_O^X AND e_O^X AT ABOUT 1600°C

From figure 15, it is seen that the value of e_O^{Cr} obtained from this investigation is not inconsistent with Ohtani and Gokcen's (54) idea of periodicity. By means of the foregoing correlations it is possible to make approximate predictions of the parameters of elements for which there are no experimental results.

2. The Effect of Oxygen on the Activity Coefficient of Chromium

The effect of oxygen on the activity coefficient of chromium can be calculated from Wagner's reciprocity relation given in equation (11) which in this case takes the form

$$e_O^{Cr} = \frac{M_O}{M_{Cr}} e_{Cr}^O$$

and

$$e_{Cr}^O = \frac{52}{16} \times (-0.068)$$

$$= (-0.221)$$

so that

$$\log f_{Cr}^O = -0.221 \ (\%\ O) \quad \text{at } 1585°C \tag{59}$$

3. The Effect of Temperature on the Interaction Parameter

In the temperature range examined, 1516° to 1726°C, it was not possible in the present investigation to determine the effect of temperature on the interaction parameter. It is probable that the temperature effect is slight as shown by the work of Turkdogan (33) Matoba and Kuwana (20) and the present investigation. Although the temperature effect is small, it should not be zero and the value of the parameter e_O^{Cr} should decrease with increasing temperature. In figure 16 a plot of e_O^{Cr} against the reciprocal of the absolute temperature is presented. Also shown in the figure are results of several other investigators.

The work of Bell and co-workers (35, 36) suggests that there is

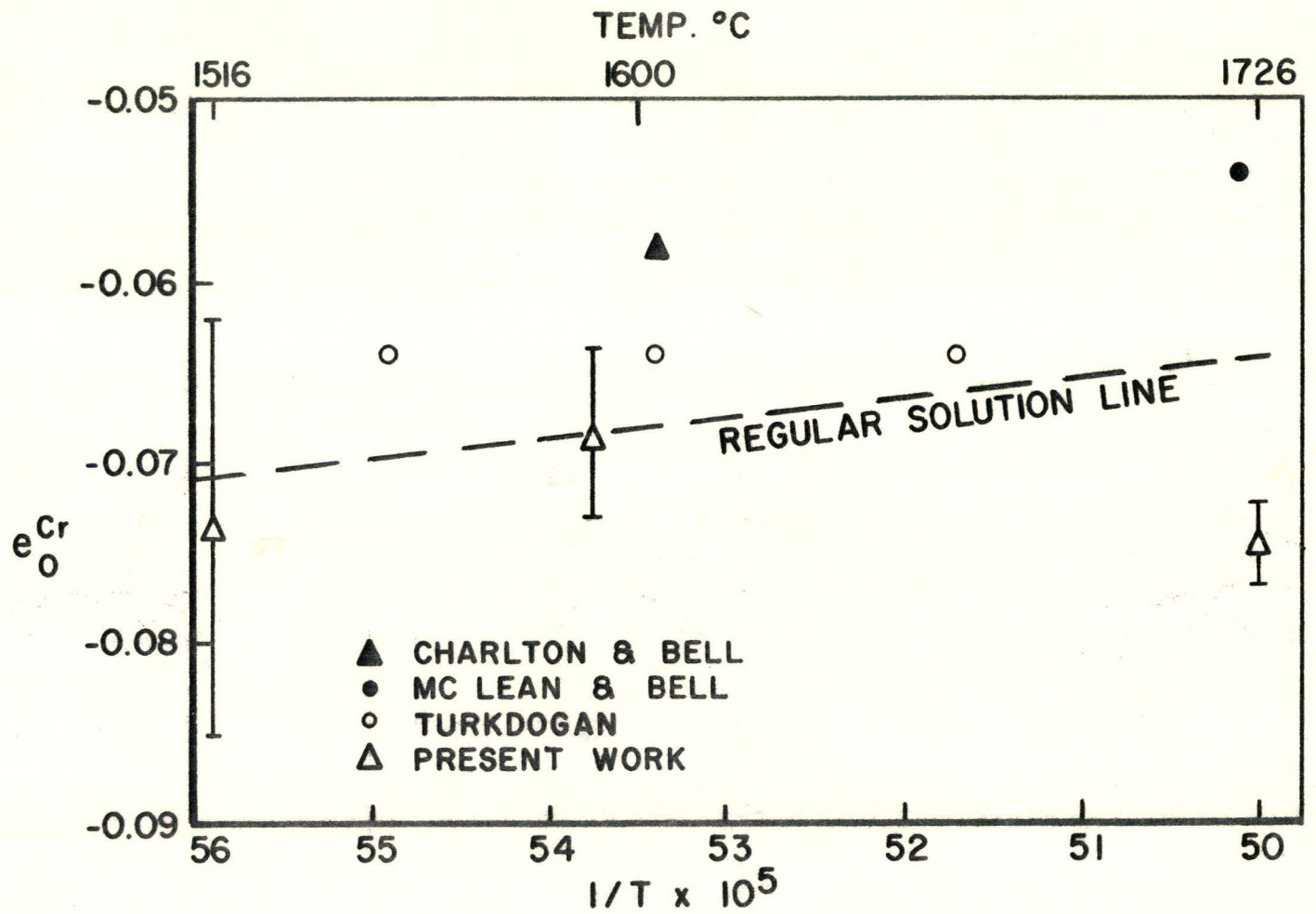
TEMP. °C
1516
1600
1726
-0.05
-0.06
-0.07
-0.08
-0.09
e_O^{Cr}
REGULAR SOLUTION LINE
CHARLTON & BELL
MC LEAN & BELL
TURKDOGAN
PRESENT WORK
56
55
54
53
52
51
50
1/T x 10^5

FIGURE 16

a reciprocal relation between e_O^{Cr} and the absolute temperature in dilute iron-chromium alloys. A possible explanation of this observation is that such solutions are regular. If the solution is regular then the entropy interaction parameter s_O^{Cr} is zero and equation (23) reduces to the form

$$e_O^{Cr} = \frac{h_O^{Cr}}{4.575T}$$

and a reciprocal relation between e_O^{Cr} and absolute temperature is the result. This regular solution line is plotted as a dotted line in figure 16 through the experimental value of e_O^{Cr} at 1585°C.

4. Prediction of the Heat of Solution of Oxygen into Dilute Iron-Chromium Alloys

Consider the oxygen solution reaction

$$\frac{1}{2} O_2 = \underline{O} \tag{40}$$

where

$$K = \frac{f_O \, (\% O)}{p_{O_2}^{1/2}} \tag{60}$$

For oxygen solution into an iron-chromium alloy

$$K = \frac{f_O^{Cr} \, (\% O)}{p_{O_2}^{1/2}}$$

where f_O^O is assumed to be unity

Now

$$K' = \frac{(\%\ O)}{P_{O_2}^{1/2}} \tag{61}$$

so that

$$\log K = \log K' + \log f_O^{Cr}$$

and

$$\log K' = \log K - \log f_O^{Cr}$$

$$= \log K - e_O^{Cr}\ (\%\ Cr) \tag{62}$$

Now substitute the relations $\log K = -\frac{\Delta G^O}{4.575T} = -\frac{\Delta H^O}{4.575T} + \frac{\Delta S^O}{4.575}$ and equation (23) into (62).

Then

$$\log K' = -\frac{\Delta H^O}{4.575T} + \frac{\Delta S^O}{4.575} - \frac{h_O^{Cr}\ (\%\ Cr)}{4.575T} + \frac{s_O^{Cr}\ (\%\ Cr)}{4.575}$$

by rearrangement

$$\log K' = -\frac{1}{4.575T}\left(\Delta H^O + h_O^{Cr}\ [\%\ Cr]\right) + \left(\Delta S^O + s_O^{Cr}\ [\%\ Cr]\right)\frac{1}{4.575} \tag{63}$$

The heat of solution of oxygen into liquid iron-chromium alloys is ΔH_{Cr} where

$$\Delta H_{Cr} = \Delta H^O + h_O^{Cr}\ (\%\ Cr) \tag{64}$$

and

ΔH^O is the heat of solution into pure iron

$h_O^{Cr}\ (\%\ Cr)$ is, by the formalism of Corrigan and Chipman (7), the extra enthalpy $H^{x\ Cr}_O$ for a given composition.

Similarly ΔS_{Cr} is the entropy of mixing into the alloy

$$\Delta S_{Cr} = \Delta S^{O} + s_{O}^{Cr} \ (\% \ Cr) \qquad (65)$$

where

ΔS^{O} is the entropy of mixing into pure iron

s_{O}^{Cr} (% Cr) is the extra entropy $S^{x}{}_{O}^{Cr}$ for a given composition

If the regular solution line in figure 16 was assumed to be correct then the value of h_{O}^{Cr} would be - 0.58 k cal. The heat of solution of oxygen with chromium content would vary as shown in figure 17.

5. Summary

(i) Chromium lowers the activity coefficient of dissolved oxygen and the magnitude of this interaction at 1585°C is given by the relation

$$\log f_{O}^{Cr} = - 0.068 \ (\% \ Cr)$$

(ii) The reverse effect of oxygen on the activity coefficient of chromium was calculated and found to be represented by the equation

$$\log f_{Cr}^{O} = - 0.221 \ (\% \ O)$$

(iii) The effect of temperature on the interaction parameter could not be established. A method for predicting the heat of solution of oxygen into dilute iron-chromium alloys is presented which can be used if the effect of temperature on the interaction parameter e_{O}^{Cr} is established or can be assumed.

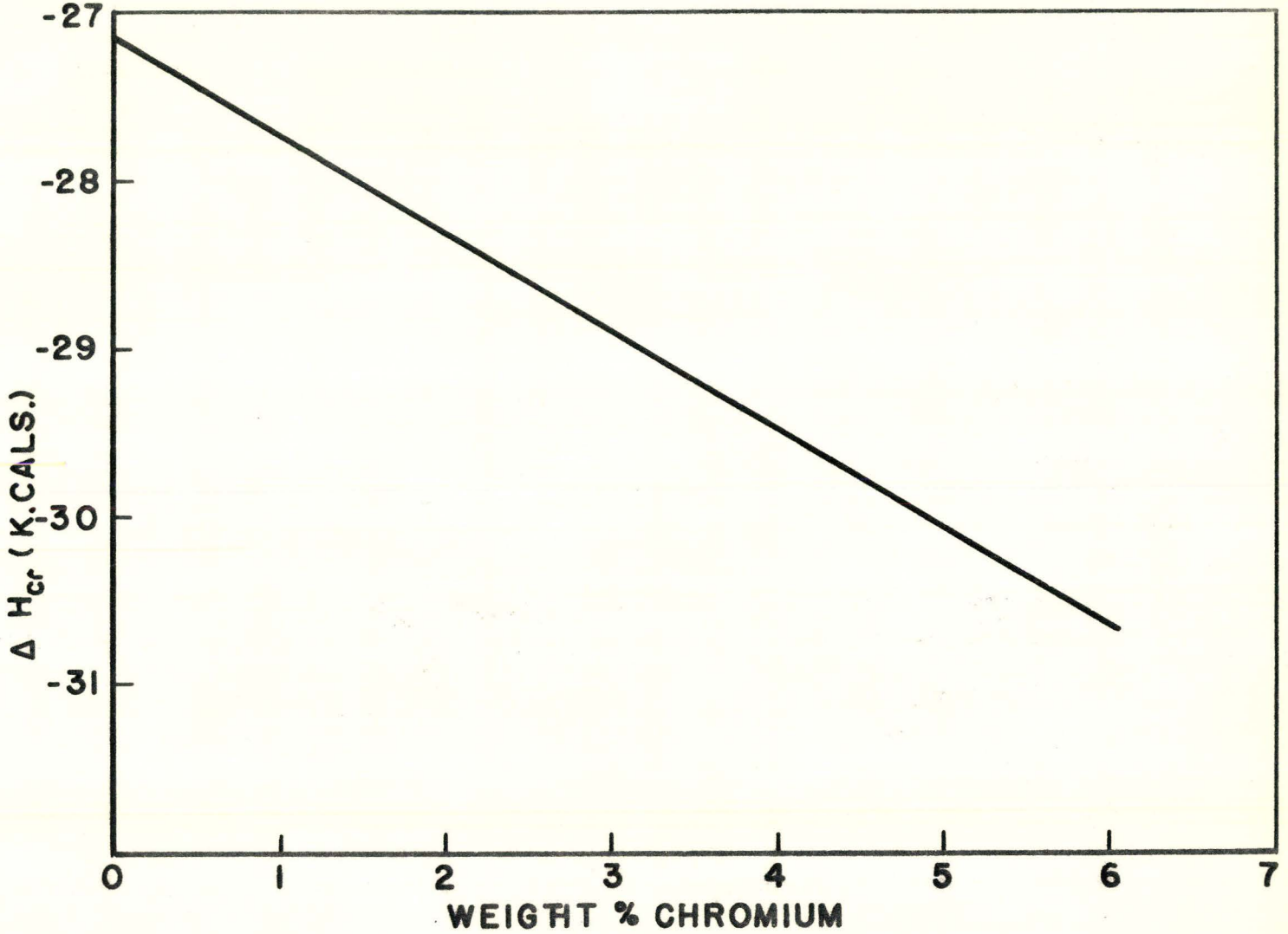

FIGURE 17

PREDICTED HEAT OF SOLUTION OF OXYGEN INTO DILUTE LIQUID IRON-CHROMIUM ALLOYS

BIBLIOGRAPHY

1. J. Chipman, C. W. Sherman, Trans. A.I.M.E., (1950), 188, 334.
2. C. Wagner, Thermodynamics of Alloys, Addison Wesley Press, (1952), 51 - 53.
3. H. Schenck, M. G. Frohberg and E. Steinmetz, Arch Eisenhuettenw, (1960), 31, 671.
4. C. Lupis and J. F. Elliott, Trans. Met. Soc. A.I.M.E., (1965), 233, 257 - 58.
5. C. Lupis and J. F. Elliott, Trans. Met. Soc. A.I.M.E., (1965), 233, 829 - 30.
6. P. N. Smith and I. S. R. Clark, M.Sc. Theses, McMaster University, 1965.
7. J. Chipman and D. A. Corrigan, Trans. Met. Soc. A.I.M.E., (1965), 233, 1249 - 51.
8. L. S. Darken and R. W. Gurry, Physical Chemistry of Metals, McGraw-Hill Book Co., (1953).
9. J. Chipman, J. Am. Chem. Soc., (1933), 55, 3131.
10. J. G. Thompson, H. C. Vacher and H. A. Bright, Trans. A.I.M.E., (1937), 125, 246.
11. M. G. Fontana and J. Chipman, Trans. A.S.M., (1936), 24, 313.
12. J. Chipman and A. M. Samarin, Trans. A.I.M.E., (1937), 125, 331.
13. M. N. Dastur and J. Chipman, Trans. A.I.M.E., (1949), 185, 441.
14. N. A. Gokcen, Trans. A.I.M.E., (1956), 206, 1558.
15. T. P. Floridis and J. Chipman, Trans. Met. Soc. A.I.M.E., (1958), 212, 549.

16. E. S. Tankins, N. A. Gokcen and G. R. Belton, Trans. Met. Soc. A.I.M.E., (1964), 230, 820 - 27.

17. S. Matoba, Anniversary Volume, Tohoku Imperial University, Japan, (1936), p. 548.

18. V. V. Averin, A. Y. Polyakov, and A. M. Samarin, Izv. Akad. Nauk. S.S.S.R., Otd. Tekhn. Nauk, (1955), 3, p. 90.

19. H. A. Wreidt and J. Chipman, Trans. A.I.M.E., (1955), 203, 477.

20. S. Matoba and T. Kuwana, Tetsu-to-Hagane, (1965), 5, No. 3, 187 - 195.

21. N. A. Gokcen and J. Chipman, Trans. A.I.M.E., (1952), 195, 171.

22. H. Sakao and K. Sano, Trans. Japan Inst. Metals, (1960), 1, 38 - 42.

23. S. Matoba and Y. Gunji, Nihon Gakujutsu Shinkokai, 19th Committee Report, April (1959), No. 5425.

24. P. H. Emmet and J. F. Schultz, J. Am. Chem. Soc., (1933), 55, 1376.

25. L. S. Darken and R. W. Gurry, J. Am. Chem. Soc., (1945), 67, 1398.

26. M. N. Dastur and J. Chipman, Disc. Faraday Soc., (1948), 4, 100.

27. J. Bockris, J. White and J. Mackenzie, Physicochemical Measurements at High Temperatures, Butterworths Scientific Publications, (1959).

28. J. C. D'Entremont, Trans. Met. Soc. A.I.M.E., (1963), 227, 482.

29. P. Kosakevitch and G. Urbain, Mem. Sci. Rev. Met., (1961), 58, 401.

30. H. Chen and J. Chipman, Trans. A.S.M., (1947), 38, 70 - 113.

31. J. Chipman, J.I.S.I., (1955), 180, 97.

32. B. V. Linchevskii and A. M. Samarin, Izvest. Akad. Nauk. S.S.S.R., Otdel. Tekn. Nauk., (1953), 5, 691.

33. E. T. Turkdogan, J. Iron Steel Inst., (1954), 178, 278.

34. H. Sakao and K. Sano, J. Japan Inst. Met., (1962), vol. 26, 4, 236 - 244.

35. K. Charlton, Ph.D. Thesis, R.C.S.T. Glasgow, (1963).

36. A. McLean and H. B. Bell, J.I.S.I., (1965), 203, 123 - 30.

37. L. Enskog, Physik Z, (1911), 12, 56 and 533.

38. S. Chapman, Phil. Trans. Roy. Soc. A., (1916), 216, 279, (1917), 217, 110.

39. S. Chapman and F. Dootson, Phil. Mag., (1917), 33, 248.

40. L. J. Gillespie, J. Chem. Physics, (1939), 7, 530.

41. J. Bockris, J. White and J. Mackenzie, Physicochemical Measurements at High Temperature, Butterworths Publications, (1959), pp. 137 - 171.

42. C. B. Alcock, International J. Appl. Radiation and Isotopes, (1958), 3, 401.

43. W. A. Peifer, Journal of Metals, (1965), 17, 487 - 493.

44. B. Harris, A. E. Jenkins, Private Communication.

45. B. Harris, A. E. Jenkins, Jour. Sc. Instr., (1959), 36, 238 - 239.

46. A. E. Jenkins, B. Harris and L. Baker, Symposium on Metallurgy at High Pressures and High Temperatures, Met. Soc. A.I.M.E. Conference, 22, 23 - 43.

47. F. H. Schofield and A. Grace, 8th Report on Heterogeneity of Steel Ingots, Iron and Steel Inst. Spec. Report, (1939), No. 25.

48. H. C. Vacher, Journal of Research, U.S. Bureau of Standards, (1933), 11, 541.

49. G. Phragmen and B. Kalling, Jernkontorets Annaler., (1939), 123, 199.

50. S. Marshall and J. Chipman, Trans. A.I.M.E., (1940), 140, 127.

51. J. Chipman and K. Fetters, Trans. A.S.M., (1941), 29, 955.

52. C. R. Taylor and J. Chipman, Trans. A.I.M.E., (1943), 154, 228.

53. L. S. Darken and R. W. Gurry, Journ. Am. Chem. Soc., (1945), 67; (1946), 68, 798.

54. M. Ohtani and N. A. Gokcen, Trans. Met. Soc. A.I.M.E., (1960), 218, 533.

55. J. V. Quagliano, Chemistry, Prentice-Hall Inc., (1958).

56. S. Marshall and J. Chipman, Trans. A.S.M., (1942), 30, 695.

57. N. A. Gokcen and J. Chipman, Trans. A.I.M.E., (1953), 197, 173.

58. N. A. Gokcen and J. Chipman, Trans. A.I.M.E., (1953), 197, 1017.

59. J. Pearson and E. T. Turkdogan, J.I.S.I., (1954), 176, 19.

60. S. Matoba and T. Uno, Tetsu to Hagane, (1942), 28, 651.

61. M. N. Dastur and J. Chipman, Trans. A.I.M.E., (1949), 185, 441; (1951), 191, 14.

62. J. Thiery, Dissertation, M.I.T.

63. H. A. Wreidt and J. Chipman, Trans. A.I.M.E., (1956), 206, 1195.

64. T. Fuwa and J. Chipman, Trans. Met. Soc. A.I.M.E., (1960), 218, 887.